

# Efficient and Adaptive Estimation of Local Triadic Coefficients

Ilie Sarpe

KTH Royal Institute of Technology  
Stockholm, Sweden  
ilsarpe@kth.se

Aristides Gionis

KTH Royal Institute of Technology  
Stockholm, Sweden  
argioni@kth.se

## ABSTRACT

Characterizing graph properties is fundamental to the analysis and to our understanding of real-world networked systems. The *local clustering coefficient*, and the more recently introduced, *local closure coefficient*, capture powerful properties that are essential in a large number of applications, ranging from graph embeddings to graph partitioning. Such coefficients capture the local density of the neighborhood of each node, considering incident triadic structures and paths of length two. For this reason, we refer to these coefficients collectively as *local triadic coefficients*.

In this work, we consider the novel problem of computing efficiently the *average* of local triadic coefficients, over a given *partition* of the nodes of the input graph into a set of disjoint *buckets*. The *average local triadic coefficients* of the nodes in each bucket provide a better insight into the interplay of graph structure and the properties of the nodes associated to each bucket. Unfortunately, exact computation, which requires listing all triangles in a graph, is infeasible for large networks. Hence, we focus on obtaining *highly-accurate probabilistic estimates*.

We develop TRIAD, an adaptive algorithm based on sampling, which can be used to estimate the average local triadic coefficients for a partition of the nodes into buckets. TRIAD is based on a new class of unbiased estimators, and non-trivial bounds on its sample complexity, enabling the efficient computation of highly accurate estimates. Finally, we show how TRIAD can be efficiently used in practice on large networks, and we present a case study showing that average local triadic coefficients can capture high-order patterns over collaboration networks.

### ACM Reference Format:

Ilie Sarpe and Aristides Gionis. 2025. Efficient and Adaptive Estimation of Local Triadic Coefficients. In *Proceedings of ACM Conference (Conference'17)*. ACM, New York, NY, USA, 23 pages. <https://doi.org/10.1145/nmnnnnn.nnnnnnn>

### PVLDB Reference Format:

Ilie Sarpe and Aristides Gionis. Efficient and Adaptive Estimation of Local Triadic Coefficients. PVLDB, 18(8): 2561 - 2574, 2025. doi:10.14778/3742728.3742748

This work is licensed under the Creative Commons BY-NC-ND 4.0 International License. Visit <https://creativecommons.org/licenses/by-nc-nd/4.0/> to view a copy of this license. For any use beyond those covered by this license, obtain permission by emailing [info@vldb.org](mailto:info@vldb.org). Copyright is held by the owner/author(s). Publication rights licensed to the VLDB Endowment. Proceedings of the VLDB Endowment, Vol. 18, No. 8 ISSN 2150-8097. doi:10.14778/3742728.3742748

Conference'17, July 2017, Washington, DC, USA

© 2025 Association for Computing Machinery.

This is the author's version of the work. It is posted here for your personal use. Not for redistribution. The definitive Version of Record was published in *Proceedings of ACM Conference (Conference'17)*, <https://doi.org/10.1145/nmnnnnn.nnnnnnn>.

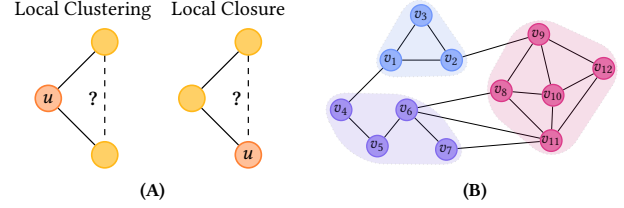


**Figure 1:** 1A: the local clustering coefficient of a node  $u$  considers the fraction of connected pairs of neighbors of  $u$ , while the local closure coefficient of  $u$  considers the fraction of neighbors of  $u$ 's neighbors to which  $u$  is connected. 1B: a graph with its set of nodes partitioned into three different sets.

### PVLDB Artifact Availability:

The source code, data, and/or other artifacts have been made available at <https://github.com/iliesarpe/Triad>.

## 1 INTRODUCTION

Graphs are a ubiquitous data abstraction used to study complex systems in different domains, such as social networks [18], protein interactions [8], information networks [57], and more [37]. A graph provides a simple representation: entities are represented by nodes and their relations are represented by edges, enabling the analysis of structural properties and giving unique insights into the function of various systems [64]. For example, flow analysis in transport graphs can be used for better urban design [21], subgraph patterns can improve recommenders [29]; and dense subgraph identification captures highly collaborative communities [32].

The *local clustering coefficient* [61] is among the most important structural properties for graph analysis, and is used in many applications related to databases [14], social networks [19], graph embeddings [9], and link prediction [63]. The local clustering coefficient measures the fraction of connected pairs of neighbors of a given node  $u$ , e.g., see Figure 1A (left), providing a simple and interpretable value on how well the node is “embedded” within its local neighborhood. On an academic collaboration network, for example, the local clustering coefficient of an author  $u$  corresponds to the fraction of the coauthors of  $u$  collaborating with each other, capturing a salient coauthorship pattern of author  $u$ .

Recently, Yin et al. [66] introduced the *local closure coefficient*, a new coefficient capturing the fraction of paths of length two, originating from a node  $u$  that is closed by  $u$ , e.g., see Figure 1A (right). This novel definition directly accounts for the connections generated by  $u$  in the graph, differently from the local clustering coefficient that only depends on connections in  $u$ 's neighborhood. The local closure coefficient is a simple concept that is gaining

interest in the research community, as it provides additional and complementary insights to existing coefficients and has applications in anomaly detection [69] and link prediction [66]. In this paper, we refer collectively to the local clustering coefficient and the local closure coefficient as *local triadic coefficients*. Both local triadic coefficients are fundamental quantities for graph analysis, as they capture structural properties of graphs on a local level [65–67].

In several applications, we are interested in the *average* local triadic coefficient of a subset of nodes [23, 33, 59]. The most typical example is to consider the average over *all* nodes in the graph, e.g., the *average local clustering coefficient*: a standard graph statistic available in popular graph libraries [30, 45]. In general, computing the average local triadic coefficients of a *subset* of nodes based on graph properties can yield unique insights. For example, such properties may be associated with node metadata (e.g., in typed networks [53]), node similarities (e.g., from structural properties such core number and degrees, or role similarity [22]), or graph communities [24]. As a concrete example, in an academic collaboration network, we can compute the average local triadic coefficient of all authors who publish consistently in certain venues. For example, database conferences or machine learning—and average local coefficients could reveal interesting patterns for each community of interest, such as different trends in collaboration patterns.

The average local clustering coefficient is also exploited as a measure for community detection or clustering algorithms [38], with good quality clusters achieving high average local clustering coefficients, e.g., compared to random partitions. Hence, analyzing the average local triadic coefficient for different buckets can provide us with powerful insights for various applications, ranging from analyzing structural properties of specific groups of users with similar metadata, to community detection. Furthermore, average local triadic coefficients can also be employed to empower machine learning models, e.g., GNNs, for tasks such as graph classification or node embeddings [9].

Motivated by the previous settings requiring to compute the average local triadic coefficients over (given) sets of nodes, in this paper, we study the following problem: given a partition of the nodes of a graph into  $k$  sets, efficiently compute the average local triadic coefficient (clustering or closure) *for each* set of the partition.

Unfortunately, to address this problem, we cannot rely on exact algorithms, since exact computation of the local triadic coefficients for all graph nodes is an extremely challenging task and requires exhaustive enumeration of all triangles in a graph. Despite extensive study of exact algorithms for *triangle counting* [4, 5, 31], enumeration requires time  $\Theta(m^{3/2})$ , i.e.,  $\Theta(n^3)$  on dense graphs, which is extremely inefficient and resource-demanding for massive graphs.<sup>1</sup>

To overcome this challenge, we develop an efficient *adaptive approximation* algorithm: TRIAD (average local TRIAdic ADaptive estimation), which can break the complexity barrier at the expense of a small approximation error. Similar to other approximation algorithms for graph analysis, TRIAD relies on *random sampling* [11, 60, 71]. Where, triangles incident to randomly sampled edges are used to update an estimate of the average triadic coefficient *for each* set of the partition of the nodes of a graph, through a novel *class* of unbiased estimators. TRIAD can approximate both the average

local clustering and closure coefficients of arbitrary partitions of the graph nodes. Surprisingly, to the best of our knowledge, TRIAD is also the first algorithm specifically designed to estimate average local closure coefficients.

Our design of TRIAD is guided by two key properties, essential for many sampling schemes: (i) provide accurate estimates that are close to the unknown values being estimated; (ii) provide high-quality adaptive probabilistic guarantees on the distance between the estimates and the values being estimated. In fact, differently from existing approaches TRIAD quantifies the deviation between the probabilistic estimates reported in output and the underlying unknown average coefficients through a data-dependent approach [27, 28, 49, 70]. This approach results in an extremely efficient algorithm, whose performance is judiciously adapted to the input graph, since the estimation is based on empirical quantities computed over the collected samples. Our contributions are as follows.

- We study the problem of efficiently obtaining high-quality estimates of the average local closure and average local clustering coefficients for each set in a partition of the nodes of a graph.
- We develop TRIAD, an efficient and adaptive algorithm that provides high-quality estimates with controlled error probability. TRIAD is based on a novel class of estimators that we optimize to achieve provably small variance and a novel bound on the sample size obtained through the notion of pseudo-dimension. TRIAD also leverages state-of-the-art variance-aware concentration results to quantify the deviation of its estimates to the unknown estimated values, by the means of adaptive data-dependent bounds.
- We extensively assess the performance of TRIAD on large graphs. Our results show that TRIAD provides high-quality probabilistic estimates and strong theoretical guarantees not matched by existing state-of-the-art algorithms. We also show how the estimates of TRIAD can be used to study publication patterns among research fields over time on a DBLP graph.

## 2 PRELIMINARIES

Let  $G = (V, E)$  be a simple and undirected graph with node-set  $V = \{v_1, \dots, v_n\}$  and edge-set  $E = \{\{u, v\} : u \in V, v \in V \text{ and } u \neq v\}$ , where  $|V| = n$  and  $|E| = m$ .

For a node  $v \in V$  we denote its *neighborhood* with  $\mathcal{N}_v = \{u \in V : \text{it exists } \{u, v\} \in E\}$  and its *degree* with  $d_v = |\mathcal{N}_v|$ . Similarly, given an edge  $e = \{u, v\} \in E$  we define  $\mathcal{N}_e = \{w \in V : w \in (\mathcal{N}_u \cap \mathcal{N}_v)\}$ , i.e., the neighborhood of an edge  $e \in E$  is the set of nodes from  $V$  that are neighbors to *both* incident nodes of  $e$ .

A *wedge* is a set of two distinct edges sharing a common node, i.e.,  $w = \{e_1, e_2\} \subseteq E$  such that  $|e_1 \cap e_2| = 1$ ; a wedge also corresponds to a path of length two. We let  $\mathcal{W} = \{w : w \text{ is a wedge in } G\}$  be the set of all wedges in the graph  $G$ . Given a node  $v \in V$  we say that a wedge  $w = \{e_1, e_2\}$  is *centered* at  $v$  if  $\{v\} = e_1 \cap e_2$ . The set of all such wedges is denoted with  $\mathcal{W}_v^c$ . Note that, for each node  $v \in V$ , it holds  $|\mathcal{W}_v^c| = \binom{d_v}{2}$ . A wedge  $w = \{e_1, e_2\}$  is *headed* at a node  $v \in V$

<sup>1</sup>We use  $n$  and  $m$  for the number of nodes and edges respectively.

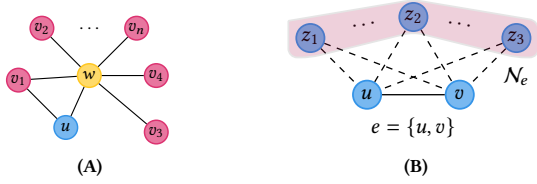


**Figure 2: 2A: Discussion in Section 2. For node  $u$  it holds  $\alpha_u = 1$  and  $\phi_u = O(1/n)$ . For node  $w$  it holds  $\alpha_w = O(1/n^2)$  and  $\phi_w = 1$ . Thus, the local clustering and local closure coefficients can differ significantly. 2B: Discussion in Section 3. Consider a sampled edge  $e \in E$ . For each node  $w \in V$  in the graph, our estimate for  $|\Delta_w|$  is  $|\Delta_w| = q|\Delta_e|/p$ , if  $w \in \{u, v\}$ , and  $|\Delta_w| = (1 - 2q)|\Delta_e|/p$ , if  $w = z_i \in N_e$ .**

if  $v \in w$  and  $v \notin e_1 \cap e_2$ .<sup>2</sup> The set of wedges headed at  $v \in V$  is denoted with  $W_v^h$ . Note that  $|W_v^h| = \sum_{u \in N_v} (d_u - 1)$ .

*Example 2.1.* In Figure 1B,  $\{v_6, v_8\}, \{v_8, v_{11}\}$  is a wedge centered at  $v_8$  and  $|W_{v_8}^c| = 6$ , since  $d_{v_8} = 4$ . Additionally,  $\{v_2, v_9\}, \{v_9, v_8\}$  is a wedge headed at  $v_8$  and  $|W_{v_8}^h| = 13$ .

Next, given a graph  $G = (V, E)$  we define a *triangle* as a set of three edges that pairwise share an edge, i.e.,  $\delta = \{\{u, v\}, \{v, w\}, \{w, u\}\} \subseteq E$  and  $u, v, w \in V$  are three distinct nodes. The set of all triangles in  $G$  is denoted by  $\Delta = \{\delta : \delta \text{ is a triangle in } G\}$ , while  $\Delta_v = \{\delta \in \Delta : v \in \delta\} \subseteq \Delta$ ,<sup>3</sup> corresponds to the set of triangles containing  $v \in V$ . Similarly  $\Delta_e = \{\delta \in \Delta : e \in \delta\}$  corresponds to the set of all triangles containing an edge  $e \in E$ .

We are now ready to introduce the fundamental triadic coefficients studied in this paper and introduced in earlier work [61, 66].

**Definition 2.2.** Given a graph  $G = (V, E)$  and a node  $v \in V$  we define the *local clustering coefficient* of  $v$ , denoted by  $\alpha_v$ , and the *local closure coefficient* of  $v$ , denoted by  $\phi_v$ , respectively as

$$\alpha_v = \frac{|\Delta_v|}{|W_v^c|} = \frac{|\Delta_v|}{\binom{d_v}{2}} \quad \text{and} \quad \phi_v = \frac{2|\Delta_v|}{|W_v^h|} = \frac{2|\Delta_v|}{\sum_{u \in N_v} (d_u - 1)}.$$

As an example, consider  $v_9$  in Figure 1B. Then  $\alpha_{v_9} = 2/(2 \cdot 3) = 1/3$  and  $\phi_{v_9} = (2 \cdot 2)/10 = 2/5$ .

Observe that the values of  $\alpha_v$  and  $\phi_v$  for a node  $v \in V$  can differ significantly, as illustrated in the example of Figure 2A.

Next, given a subset of nodes  $V' \subseteq V$  we define the *average local clustering coefficient* (respectively, *average local closure coefficient*) as the average of the local clustering (respectively, local closure) coefficient of the nodes in the subset  $V'$ , that is  $\alpha(V') = \frac{1}{|V'|} \sum_{v \in V'} \alpha_v$  (respectively,  $\phi(V') = \frac{1}{|V'|} \sum_{v \in V'} \phi_v$ ).

Given a set  $A \neq \emptyset$ , then  $A_1, \dots, A_k$  is a partition of  $A$  if  $A_i \cap A_j = \emptyset$  for  $i \neq j$  with  $i, j \in [k]$ ,  $A_i \neq \emptyset$  for all  $i \geq 1$ , and  $\bigcup_{i \geq 1} A_i = A$ . For ease of notation we denote a partition of  $V$  into  $k$  sets as  $\mathcal{V}$ . In Figure 1B we illustrate a network and a partition of the set of nodes. For ease of notation we use  $\psi_v$  to refer to a local triadic coefficient of a node  $v \in V$  (that is, either clustering coefficient or closure coefficient) and  $\Psi(V') = \frac{1}{|V'|} \sum_{v \in V'} \psi_v$ .

<sup>2</sup>We write  $v \in w = \{e_1, e_2\}$  to denote that  $v \in e_1$  or  $v \in e_2$ .

<sup>3</sup>We write  $v \in \delta$  to denote that there exists an edge  $e \in \delta$  such that  $v \in e$ .

Following standard ideas in the literature for controlling the quality of an approximate estimate [25, 43, 44], we consider two key properties: (i) the estimate should be close to the actual value; and (ii) there should exist rigorous guarantees quantifying the distance of the estimate to the unknown coefficient. These desirable properties are captured by the following problem formulation.

**PROBLEM 1.** Given a graph  $G = (V, E)$ , a partition  $\mathcal{V}$  of the node-set  $V$ , a local triadic coefficient  $\psi \in \{\alpha, \phi\}$ , and parameters  $(\epsilon_j)_{j=1}^k \in (0, 1)$  and  $\eta \in (0, 1)$ , obtain:

(A) Estimates  $f(V_j)$ , for  $j = 1, \dots, k$ , such that

$$\mathbb{P} \left[ \sup_{j=1, \dots, k} \left| f(V_j) - \frac{1}{|V_j|} \sum_{v \in V_j} \psi_v \right| \geq \epsilon_j \right] \leq \eta.$$

(B) Tight confidence intervals  $C_j$  as possible, where  $C_j = [f(V_j) - \hat{\epsilon}_j, f(V_j) + \hat{\epsilon}_j]$ , for  $j = 1, \dots, k$ , with  $|C_j| = 2\hat{\epsilon}_j \leq 2\epsilon_j$ , such that over all  $k$  partitions it holds

$$\mathbb{P} \left[ \frac{1}{|V_j|} \sum_{v \in V_j} \psi_v \in C_j \right] \geq 1 - \eta.$$

To simplify our notation and when it is clear from the context we write  $f_j$  instead of  $f(V_j)$  and  $\Psi_j$  instead of  $\Psi(V_j)$ , for  $j \in [k]$ .

In the remaining of this section we discuss the formulation of Problem 1. In particular, Problem 1 takes as input a graph  $G$  and a node partition  $\mathcal{V}$ . The goal is to obtain *accurate* estimates  $f_j$ , within at most  $\epsilon_j$  *additive error* (i.e.,  $|f_j - \Psi_j| \leq \epsilon_j$ ) for the local triadic coefficients  $\Psi_j$  with controlled error probability ( $\eta$ ) *over all sets  $j \in [k]$*  of the partition  $\mathcal{V}$ . This requirement is enforced with condition (A) in Problem 1.

Furthermore, condition (B) ensures that the confidence intervals  $C_j$  (i.e., the ranges in which the values  $\Psi_j$  are likely to fall) centered around  $f_j$  are small. This requirement provides a rigorous guarantee on the proximity of  $f_j$ 's to the corresponding  $\Psi_j$ 's.

Note that Problem 1 allows the user to provide non-uniform error bounds  $\epsilon_j$ ,  $j = 1, \dots, k$ . This flexibility is highly desirable since (i) there may be partitions for which estimates are required with different levels of precision (as controlled by  $\epsilon_j$ ), e.g., in certain applications the user may require higher precision on the value of  $\Psi_j$  for some  $j$ 's, and (ii) different values of  $\epsilon_j$  may be required to distinguish between the values of  $\Psi_j$  for different sets in  $\mathcal{V}$  [10, 41].

To clarify point (ii) above, consider  $V = V_1 \cup V_2$  with  $\Psi_1 = 10^{-2}$  and  $\Psi_2 = 10^{-5}$ . If  $\epsilon = \epsilon_1 = \epsilon_2 = 5 \cdot 10^{-2}$  then both  $f_1, f_2 \in [0, \epsilon]$  satisfy the guarantees of Problem 1 but this does not allow to distinguish between the very large value difference of  $\Psi_1$  and  $\Psi_2$  (i.e., three orders of magnitude). On the other hand, by allowing different accuracy levels, e.g.,  $\epsilon_1 = 10^{-3}$  and  $\epsilon_2 = 10^{-4}$ , we can address the issue. The acute reader may notice in this example we assume that we know the values of  $\Psi_1$  and  $\Psi_2$  in advance, and we set the values  $\epsilon_j$ 's accordingly, while in practice this is rarely the case. However, as we show in Section 3, our algorithm TRIAD can adaptively address the case of unknown  $\Psi_j$ 's.

An alternative approach would be to require *relative error guarantees*, i.e.,  $|f_j - \Psi_j| \leq \epsilon_j \Psi_j$ , for all  $j \in [k]$ . Unfortunately this problem cannot be solved efficiently. First, it requires a lower bound on each value  $\Psi_j$ , and second it requires an impractical number of

samples even for moderate values of  $\Psi_j$  and  $\varepsilon_j$ . In particular, state-of-the-art methods [15, 28, 49, 70] have shown that  $\Omega(1/(\varepsilon\Psi_j)^2)$  samples may be needed. Thus, if, say,  $\Psi = 10^{-3}$  and  $\varepsilon = 10^{-2}$ , then  $\Omega(10^{10})$  samples would be needed, resulting in an extremely high and impractical running time.

### 3 METHODS

Our algorithm TRIAD consists of several components. At its core, it is based on a new class of unbiased estimators, which can be of independent interest for local triangle count estimation. We discuss these estimators in Section 3.1. We then introduce TRIAD, in Section 3.2. We present TRIAD's analysis in Section 3.3, and some practical optimizations in Section 3.4. We analyze the time and memory complexity of TRIAD in Section 3.5. Finally, in Section 3.6 we discuss the adaptive behavior of TRIAD. All missing proofs are reported in Appendix A.

#### 3.1 New estimates for local counts

We introduce a new *class* of estimators to approximate, for each node  $v \in V$ , the number of triangle counts  $|\Delta_v|$  (i.e., locally to  $v$ ), based on a simple sampling procedure that uniformly selects random edges. Such estimators stand at the core of the proposed method TRIAD, enabling a small variance of the estimates in output.

To compute the estimators for  $|\Delta_v|$ , for  $v \in V$ , first we sample uniformly an edge  $e \in E$ , and then collect the set of triangles  $\Delta_e$ . The total number of triangles  $|\Delta_e|$  is then used to estimate  $|\Delta_v|$ , for each node  $v \in V$ . The key, is in *how* the value  $|\Delta_e|$  is distributed over all nodes  $v \in e \cup \mathcal{N}_e$ , to obtain an unbiased estimators of  $|\Delta_v|$ .

In particular, our estimators distribute the weight  $|\Delta_e|$  *asymmetrically* across the nodes  $v \in e$  (where  $e \in E$  is the sampled edge) and the nodes  $v \in \mathcal{N}_e$ . This asymmetric assignment can be made before evaluating the estimates of  $|\Delta_v|$ , enabling us to obtain estimates with extremely small variance, as we show in Section 4.4.2, and discuss theoretically in Section 3.3.3.

*Example 3.1.* Consider Figure 2B, fix  $q \in [0, 1/2]$ , and suppose that  $e = \{u, v\}$  is sampled. Then the estimators of  $|\Delta_{z_i}|$  assign value  $(1-2q)/p$  for all nodes  $z_i \in \mathcal{N}_e$ , and value  $q|\Delta_e|/p$  for nodes  $u, v \in e$ , where  $p$  is the sampling probability of edge  $e$ .<sup>4</sup>

We will now show that the proposed estimates are unbiased with respect to  $|\Delta_v|$ , for all  $v \in V$ , and *any* value  $q \in [0, 1/2]$ .

LEMMA 3.2. *For any value of the parameter  $q \in [0, 1/2]$ ,*

$$X_q(v) = \sum_{e \in E: v \in e} \frac{q|\Delta_e|X_e}{p} + (1-2q) \sum_{e \in E: v \in \mathcal{N}_e} \frac{X_e}{p} \quad (1)$$

*is an unbiased estimator of  $|\Delta_v|$  for  $v \in V$ . That is,  $\mathbb{E}[X_q(v)] = |\Delta_v|$ , where the expectation is taken over a randomly sampled edge  $e \in E$ , and  $X_e$  is a 0–1 random variable indicating if  $e \in E$  is selected.*

Note that the estimator in Lemma 3.2 allows to flexibly select the parameter  $q$ , to minimize the variance of the estimates  $X_q(v)$ , for  $v \in V$ , leading to very accurate estimates with small variance when  $q$  is selected properly (see Section 3.3.3). We next use the result of Lemma 3.2 to obtain estimates  $f_i(e) : E \mapsto \mathbb{R}_0^+$  of  $\Psi_i$

<sup>4</sup>In our analysis we consider  $p = 1/m$ , but any importance sampling probability distribution  $p_e$  over  $e \in E$  can be used, provided that  $p_e > 0$  if  $|\Delta_e| > 0$ .

for each set  $V_i$ , with  $i \in [k]$ , of the partition  $\mathcal{V}$  by sampling a random edge  $e \in E$ . First, to unify our notation, given a node  $v \in V$  let  $|\mathcal{W}_v^*| = |\mathcal{W}_v^c|$  if  $*$  = c, and  $|\mathcal{W}_v^*| = |\mathcal{W}_v^h|/2$  if  $*$  = h. We can then write  $\psi_v = |\Delta_v|/|\mathcal{W}_v^*|$ , i.e.,  $\psi_v = \alpha_v$  corresponds to the local clustering coefficient if  $*$  = c and  $\psi_v = \phi_v$  otherwise. Using this notation, we have the following.

LEMMA 3.3. *Let  $e \in E$  be an edge sampled uniformly from  $E$ . Then, the random variable  $f_j(e) : E \mapsto \mathbb{R}_0^+$  defined by*

$$f_j(e) = \sum_{e \in E} \frac{X_e}{p} \frac{1}{|V_j|} \sum_{v \in V_j} \frac{a_q(v, e)}{|\mathcal{W}_v^*|},$$

*where*

$$a_q(v, e) = q|\Delta_e|1[v \in e] + (1-2q)1[v \in \mathcal{N}_e], \quad (2)$$

*is an unbiased estimate of  $\Psi_j$  for each set  $V_j \in \mathcal{V}$ ,  $j \in [k]$ , i.e.,  $\mathbb{E}[f_j(e)] = \Psi_j$ . Here,  $X_e$  is a 0–1 random variable indicating if  $e \in E$  is sampled, and  $|\mathcal{W}_v^*| = |\mathcal{W}_v^c|$  for  $\psi = \alpha$ , and  $|\mathcal{W}_v^*| = |\mathcal{W}_v^h|/2$  if  $\psi = \phi$ .*

The proof can be found in Appendix A.

Lemma 3.3 shows that by sampling a single random edge  $e \in E$  we can obtain an unbiased estimate of multiple coefficients  $\Psi_j$  associated sets  $V_j \in \mathcal{V}$ , by accurately weighting the triangles in  $\Delta_e$ . This allows to *simultaneously* update the estimates of multiple buckets  $V_j$ , for  $j \in [k]$ , differently from existing approaches [25, 49, 70], where each triangle identified by the algorithm is used to estimate the coefficient of a *single* partition.

#### 3.2 The TRIAD algorithm

Algorithm 1 presents TRIAD. The algorithm first initializes  $|\mathcal{W}_v^*|$  for each  $v \in V$  according to the coefficients  $\psi$  to be estimated (lines 1–2). TRIAD then proceeds to initialize the variables  $f_j$ , for  $j = 1, \dots, k$ , corresponding to the estimates of  $\Psi_j$  to be output (line 3). It then sets  $\varepsilon$  to the smallest  $\varepsilon_j$ , for  $j \in [k]$  (i.e.,  $\varepsilon$  is the smallest upper bound  $\varepsilon_j$  required by the user, see Problem 1). TRIAD then selects the best value of the parameter  $q \in [0, 1/2]$  to guarantee a fast termination of TRIAD by solving a specific optimization problem (line 4, subroutine `Fixq`, see Section 3.3.3). Intuitively, the value of  $q$  is fixed such that the maximum variance of  $f_j$ , for  $j \in [k]$ , is minimized, yielding a fast convergence of TRIAD. In fact, as we will show, the termination condition of TRIAD considers the *empirical* variance of the estimates  $f_j$ , over the sampled edges.

The function `UpperBounds` (line 5) computes  $R_j$ , for  $j = 1, \dots, k$ , corresponding to bounds to the maximum value that a random variable  $f_j(e)$  can take over a randomly sampled edge  $e \in E$ , i.e.,  $f_j(e) \leq R_j$  almost surely, for each  $j \in [k]$ . In addition `UpperBounds` computes  $\zeta$ , an upper bound on the pseudo-dimension of the functions  $f_j(e)$ ,  $j \in [k]$ . We use  $\zeta$  and  $R = \max_j R_j$  (line 6) to obtain a bound on the maximum number of samples  $s_{\max}$  to be explored by TRIAD (line 7). We discuss the function `UpperBounds`, and prove the bound on the sample-size in Sections 3.3.4 and 3.3.1, respectively.

Auxiliary variables are then initialized (line 6): index  $i$  keeps track of the iterations,  $\mathcal{S}$  maintains the bag of sampled edges processed,  $s$  counts the number of samples processed, and  $\eta_0$  is used to obtain the probabilistic guarantees of TRIAD. Finally,  $s_0$  corresponds to the initial sample size, i.e., the minimum sample size for which TRIAD can provide tight guarantees (line 7), that we discuss in Section 3.3.2.

---

**Algorithm 1: TRIAD**


---

**Input:**  $G = (V, E)$ ,  $(\varepsilon_j)_{j=1}^k$ ,  $\eta$ , partition  $\mathcal{V}$ ,  $\psi \in \{\alpha, \phi\}$ .  
**Output:** Estimates  $f_j$  and bounds  $\widehat{\varepsilon}_j$  s.t.  $|f_j - \Psi_j| \leq \widehat{\varepsilon}_j \leq \varepsilon_j$  for each  $j \in [k]$  w.p.  $> 1 - \eta$ .

```

1 if  $\psi = \alpha$  then  $|\mathcal{W}_v^*| \leftarrow |\mathcal{W}_v^0|$  for  $v \in V$ ;
2 else  $|\mathcal{W}_v^*| \leftarrow |\mathcal{W}_v^0|/2$  for  $v \in V$ ;
3  $f_j \leftarrow 0$  for each  $j \in [k]$ ;
4  $q \leftarrow \text{Fixq}(G, \mathcal{V})$ ;  $\varepsilon \leftarrow \min\{\varepsilon_j\}$ ;
5  $\zeta, R_1, \dots, R_k \leftarrow \text{UpperBounds}(G, \mathcal{V}, |\mathcal{W}_v^*|_{v \in V}, q)$ ;
6  $i \leftarrow 0$ ;  $\mathcal{S} \leftarrow \emptyset$ ;  $s \leftarrow 0$ ;  $\eta_0 \leftarrow \eta/2$ ;  $R \leftarrow \max\{R_j, j \in [k]\}$ ;
7  $s_{\max} \leftarrow \frac{R^2}{\varepsilon^2}(\zeta + \log(1/\eta))$ ;  $s_0 \leftarrow \lceil R \frac{3 \log(4k/\eta_0)}{\varepsilon} + 1 \rceil$ ;
8 while not  $\text{StoppingCondition}(s_{\max}, s, (f_j)_{j \geq 1}, \varepsilon)$  do
9    $\mathcal{S}_i \leftarrow \text{UniformSample}(E, s_i)$ ;
10  foreach  $e = (u, v) \in \mathcal{S}_i$  do
11    foreach  $w \in \mathcal{N}_e$  do
12       $f_j(e) \leftarrow f_j(e) + \frac{(1-2q)}{|\mathcal{W}_w^*|}$  such that  $w \in V_j$ ;
13       $f_j(e) \leftarrow f_j(e) + \frac{q|\Delta_e^u|}{|\mathcal{W}_u^*|}$  such that  $u \in V_j$ ;
14       $f_j(e) \leftarrow f_j(e) + \frac{q|\Delta_e^v|}{|\mathcal{W}_v^*|}$  such that  $v \in V_j$ ;
15   $s \leftarrow s + s_i$ ;  $\mathcal{S} \leftarrow \mathcal{S} \cup \mathcal{S}_i$ ;
16   $f_j \leftarrow \frac{m}{s|V_j|} \sum_{e \in \mathcal{S}} f_j(e)$  for each  $j = 1 \dots, k$ ;
17   $\widehat{\varepsilon}_j \leftarrow \text{ComputeEmpiricalBound}(\mathcal{F}, \mathcal{S}, \eta_i)$ ;
18   $i \leftarrow i + 1$ ;  $\eta_i \leftarrow \eta_{i-1}/2$ ;
19 return  $(f_j, \widehat{\varepsilon}_j)$  for each  $j = 1 \dots, k$ ;
```

---

The main loop of TRIAD is entered in line 8. At the  $i$ -th iteration of the loop, TRIAD samples a bag of  $s_i$  edges uniformly at random (line 9), and for each edge it computes  $f_j(e)$  as defined in Lemma 3.3 (lines 12-14). Then TRIAD updates the sample size and the bag of edges processed (line 15) together with estimates  $f_j$ , for  $j \in [k]$  (line 16) invoking the function `ComputeEmpiricalBound` to compute *non-uniform bounds*  $\widehat{\varepsilon}_j$  on the deviations  $|f_j - \Psi_j|$  such that  $|f_j - \Psi_j| \leq \widehat{\varepsilon}_j$  with controlled error probability (line 17). These bounds are *empirical*, tight, and adaptive to the samples in  $\mathcal{S}$ , leveraging the variance of the estimates  $f_j(e)$ ,  $e \in \mathcal{S}$ , and the upper bounds  $R_j$ , for  $j \in [k]$  (see Sec. 3.3.2). Finally, a set of variables is computed for the next iteration, if the stopping condition of the main-loop is not met (line 18). The call to `StoppingCondition` in TRIAD returns “true” if one the following two conditions holds, which depend on the processed samples  $\mathcal{S}$ :

- (1) if  $s \geq s_{\max}$  then with probability at least  $1 - \eta/2$  it holds  $|f_j - \Psi_j| \leq \varepsilon \leq \varepsilon_j$ ;
- (2) if  $\widehat{\varepsilon}_j \leq \varepsilon_j$  then with probability at least  $1 - \eta/2$  it holds  $|f_j - \Psi_j| \leq \widehat{\varepsilon}_j \leq \varepsilon_j$ , for each  $j \in [k]$ .

When the main loop terminates TRIAD outputs  $(f_j, \varepsilon_j)$  in case (1), or  $(f_j, \widehat{\varepsilon}_j)$  in case (2), for each set  $V_j \in \mathcal{V}$ . Note that our estimation addresses both requirements of Problem 1 as we guarantee that all the estimates  $f_j$  are within  $\varepsilon_j$  distance to  $\Psi_j$ , and furthermore, we report accurate error bounds  $\widehat{\varepsilon}_j \leq \varepsilon_j$ , for all  $j \in [k]$ , as  $\Psi_j \in [f(V_j) - \widehat{\varepsilon}_j, f(V_j) + \widehat{\varepsilon}_j]$  with high probability. For example, even for as small  $\varepsilon_j$  as  $10^{-2}$  the reported adaptive guarantees of TRIAD can be at most  $\widehat{\varepsilon}_j \approx 10^{-3}$  in a few tens of seconds (see Section 4.3).

### 3.3 Analysis

In this section we present in more detail all the components of TRIAD, and we analyze its accuracy. The next lemma states that the estimates of Algorithm 1 are unbiased, which is important to prove tight concentration.

LEMMA 3.4. *For the output  $f_j$ ,  $j = 1, \dots, k$ , of Algorithm 1, it holds:*

$$\mathbb{E}[f_j] = \frac{1}{|V_j|} \sum_{v \in V_j} \psi_v = \Psi_j,$$

that is, the estimates of Algorithm 1 are unbiased, for both local triadic coefficients  $\psi \in \{\alpha, \phi\}$ .

The proof can be found in Appendix A.

Next we provide a bound for the variance of the estimates  $f_j$ , for  $j \in [k]$ , returned by TRIAD.

LEMMA 3.5. *For the estimates  $f_j$ ,  $j = 1, \dots, k$ , of Algorithm 1, it is*

$$\text{Var}[f_j] \leq \frac{1-p}{sp} \left( \frac{1}{|V_j|} \sum_{v \in V_j} \psi_v \right)^2,$$

for both local triadic coefficients  $\psi \in \{\alpha, \phi\}$ .

The proof can be found in Appendix A.

**3.3.1 Bounding the sample size.** To present the bound on the sample size (i.e.,  $s_{\max}$ ), we first introduce the necessary notation. Given a finite domain  $\mathcal{X}$  and  $\mathcal{Q} \subseteq 2^{\mathcal{X}}$  a collection of subsets of  $\mathcal{X}$ ,<sup>5</sup> a *range-space* is the pair  $(\mathcal{X}, \mathcal{Q})$ . We say that a set  $X \subseteq \mathcal{X}$  is *shattered* by the range-set  $\mathcal{Q}$ , if it holds  $\{Q \cap X : Q \in \mathcal{Q}\} = 2^X$ . The *VC-dimension*  $\text{VC}(\mathcal{X}, \mathcal{Q})$  of the range-space is the size of the largest subset  $X \subseteq \mathcal{X}$  such that  $X$  can be shattered by  $\mathcal{Q}$ . Given a family of functions  $\mathcal{F}$  from a domain  $\mathcal{H}$  with range  $[a, b] \subseteq \mathbb{R}$ , for a function  $f \in \mathcal{F}$  we define the subset  $\mathcal{Q}_f$  of the space  $\mathcal{H} \times [a, b]$  as

$$\mathcal{Q}_f = \{(x, t) : t \leq f(x)\}, f \in \mathcal{F}.$$

We then define  $\mathcal{F}^+ = \{\mathcal{Q}_f, f \in \mathcal{F}\}$  as the range-set over the set  $\mathcal{H} \times [a, b]$ . With these definitions at hand, the *pseudo-dimension*  $\text{PD}(\mathcal{F})$  of the family of functions  $\mathcal{F}$  is defined as  $\text{PD}(\mathcal{F}) = \text{VC}(\mathcal{H} \times [a, b], \mathcal{F}^+)$ . For illustrative examples we refer the reader to the literature [43, 44, 51]. In our work, the domain  $\mathcal{H}$  corresponds to the set of edges to be sampled by TRIAD to compute the estimators  $f_j = f_{\mathcal{S}, j}$ ,  $j = 1, \dots, k$ , that is,  $\mathcal{H} = E$ .<sup>6</sup> We also define the set of functions  $\mathcal{F} = \{f_{\mathcal{S}, j} : j = 1, \dots, k\}$ , which corresponds to the set containing all functions  $f_j$ ,  $j = 1, \dots, k$  in output to TRIAD.

THEOREM 3.6. *Let  $\mathcal{F}$  be the set of functions defined above with  $\text{PD}(\mathcal{F}) \leq \zeta$ , and let  $\varepsilon, \eta \in (0, 1)$  be two parameters. If*

$$|\mathcal{S}| \geq \frac{(b-a)^2}{\varepsilon^2} \left( \zeta + \log \frac{1}{\eta} \right),$$

then with probability at least  $1 - \eta$  over the randomness of the set  $\mathcal{S}$  it holds that  $|f_j - \Psi_j| \leq \varepsilon$ , for each  $j = 1, \dots, k$ .

Note that we cannot compute  $\text{PD}(\mathcal{F})$  from its definition as this requires exponential time in general, hence we now prove a tight and efficiently computable upper bound  $\zeta$  such that  $\text{PD}(\mathcal{F}) \leq \zeta$ .

<sup>5</sup>The set containing all possible subsets of  $\mathcal{X}$ .

<sup>6</sup>We write  $f_{\mathcal{S}, j}$  to explicit that a function depends on the bag of samples  $\mathcal{S}$ .

This enables us to use Theorem 3.6 and obtain a deterministic upper bound on the sample size of TRIAD (i.e.,  $s_{\max}$  in line 7).

First, let  $\chi_v = |\{V_j \in \mathcal{V} : \text{exists } u \in (\mathcal{N}_v \cup \{v\}), u \in V_j\}|$ , i.e.,  $\chi_v$  is the number of distinct sets  $V_j$ , for  $j \in [k]$  from  $\mathcal{V}$  containing a node in the set  $\mathcal{N}_v \cup \{v\}$  for a given node  $v \in V$ .

*Example 3.7.* In the following extreme cases: (i) when every node is in a distinct bucket (i.e.,  $k = n$ ) then  $\chi_v \leq d_{\max} + 1$ , for  $v \in V$ , with  $d_{\max}$  being the maximum degree of a node in  $V$ ; (ii) when each node is in the same bucket then  $\chi_v = 1$  for every node  $v \in V$ .

Now let

$$\widehat{\chi} = \max_{e=\{u,v\} \in E} \{\chi_z : z = \arg \min\{d_u, d_v\}\} . \quad (3)$$

Intuitively  $\widehat{\chi}$  corresponds to the largest number of buckets for which a sampled edge  $e \in E$  yields a non-zero value for the estimate  $f_j(e)$ . Clearly, a trivial bound is  $\widehat{\chi} \leq \min\{k, d_{\max} + 1\}$ , which can be very loose. We next present the bound on the pseudo-dimension associated to  $\text{PD}(\mathcal{F})$ , recall that  $\mathcal{F}$  corresponds to set of estimates  $f_j, j = 1, \dots, k$ , of TRIAD.

**PROPOSITION 3.8.** *The pseudo-dimension  $\text{PD}(\mathcal{F}) = \zeta$  is bounded as  $\zeta \leq \lfloor \log_2 \widehat{\chi} \rfloor + 1$ .*

The proof can be found in Appendix A.

As an example of the powerful result of Theorem 3.8 consider the following corollary.

**COROLLARY 3.9.** *Fix  $q = 0$  and take each node in a different set in  $\mathcal{V}$  (i.e.,  $k = n$ ). Let  $G$  be a star graph. Then by Theorem 3.8 it holds  $\zeta \leq 1$ .*

The proof can be found in Appendix A.

Corollary 3.9 shows that our result provides a tight bound on the pseudo-dimension associated to the family of functions  $\mathcal{F}$ . For comparison, under the setting of Corollary 3.9, then our setting maps to the one of de Lima et al. [15]. In their work, the authors prove  $\zeta \leq O(\log n)$  for the graph in Corollary 3.9, while our result states  $\zeta \leq 1$  yielding a  $O(\log n)$  improvement, which is the maximum attainable. Clearly, a smaller upper bound for  $\zeta$  implies a significantly smaller sample size required to guarantee the desired accuracy when such bound is used for Theorem 3.6.

We can further refine the bound on the pseudo-dimension when  $q = 0$  or  $q = 1/2$ , to this end let  $\widehat{\chi}' = \max_{e \in E} \{\chi'_z : z = \arg \min\{d_u, d_v\}\}$  and  $\chi'_v$  is defined as  $\chi_v$  but on  $\mathcal{N}_v$ , i.e., it does not consider the extended neighborhood  $\mathcal{N}_v \cup \{v\}$ .

**COROLLARY 3.10.** *The pseudo-dimension  $\text{PD}(\mathcal{F}) = \zeta$  is bounded by  $\zeta \leq \lfloor \log_2 \widehat{\chi}' \rfloor + 1$  when  $q = 0$ , while  $\zeta \leq 2$  for  $q = \frac{1}{2}$ .*

The proof can be found in Appendix A.

We conclude by noting that  $\widehat{\chi}$  can be efficiently computed in  $O(m)$  time complexity with a linear scan of the edges of the graph.

**3.3.2 Computing adaptive error bounds.** We detail how TRIAD leverages adaptive and variance-aware bounds to determine the distance of  $f_j$  from  $\Psi_j$ , for  $j \in [k]$ . We need a key concentration inequality.

**THEOREM 3.11 (EMPIRICAL BERNSTEIN BOUND [34, 36]).** *Let  $X_1, \dots, X_s$  be  $s$  independent random variables such that for all  $i = 1, \dots, s$ ,*

*$\mathbb{E}[X_i] = \mu$  and  $\mathbb{P}[X_i \in [a, b]] = 1$ , and  $\widehat{v} = \frac{1}{s} \sum_{i=1}^s (X_i - \bar{X}_s)^2$  where  $\bar{X}_s = \frac{1}{s} \sum_{i=1}^s X_i$ . Then,*

$$\left| \frac{1}{s} \sum_{i=1}^s X_i - \mu \right| \leq \sqrt{\frac{2\widehat{v} \log(4/\eta)}{s}} + \frac{7(b-a) \log(4/\eta)}{3(s-1)} .$$

The above theorem connects the empirical variance over the samples  $f_j(e)$  with the distance of  $f_j$  to  $\Psi_j$ , providing a powerful result. Therefore we can use Theorem 3.11 to obtain the function `ComputeEmpiricalBound`. That is, given a partition  $V_j$  and a bag of edges  $\mathcal{S}$  sampled so far, we obtain

$$\widehat{\varepsilon}_j = \sqrt{\frac{2\widehat{v}_j \log(4k/\eta_i)}{s}} + \frac{7(R_j) \log(4k/\eta_i)}{3(s-1)}$$

at iteration  $i \geq 0$ . Note that

$$\widehat{v}_j = \frac{1}{s} \sum_{e \in \mathcal{S}} (f_j(e) - \bar{f}_j)^2,$$

which can be obtained in linear time (i.e.,  $|\mathcal{S}|$ ), assuming the values of  $f_j(e)$  are retained over the iterations. The above result provides also a criterion on how to set  $s_0$ . That is,  $s_0$  should be at least  $\lceil R \frac{3 \log(4k/\eta_0)}{\varepsilon} + 1 \rceil$  (see TRIAD in line 6) in the very optimistic case that the empirical variance  $\widehat{v}_j = 0$ , for each  $j \in [k]$ . We can now prove the guarantees offered by TRIAD.

**THEOREM 3.12.** *The output of TRIAD  $(f_j, \widehat{\varepsilon}_j)$ , for  $j \in [k]$ , is such that with probability at least  $1 - \eta$  it is  $|f_j - \Psi_j| \leq \widehat{\varepsilon}_j \leq \varepsilon_j$ , simultaneously for all sets  $V_j$ , for  $j \in [k]$ .*

The proof can be found in Appendix A.

**3.3.3 Minimizing the variance.** The value of the parameter  $q$  (in the estimator from Lemma 3.3) plays a key role for TRIAD, enabling extremely accurate estimates if set properly (see Section 4.4.2). There are many criteria to select the value of  $q$ , the most natural one would be to fix  $q$  such that TRIAD processes the minimal possible sample-size to terminate its main loop. Unfortunately, we cannot optimize directly for such property.

Instead, to select the value of  $q$  we minimizing the maximum variance of the functions  $f_j$  over all  $j \in [k]$ . In fact, a smaller variance of  $f_j$  allows TRIAD to terminate its loop by processing a small number of samples. To do so, we first sample a very small bag  $\mathcal{S}$  of edges from  $E$ , and estimate the variance of the functions  $f_j$  over  $\mathcal{S}$  for each possible value of  $q$  (Algorithm 4). The variance of  $f_j$  can, in fact, be expressed as a quadratic equation in the parameter  $q$ , i.e., there exist efficiently-computable values  $A_j, B_j, C_j$  such that  $\widehat{V}_q(f_j) = A_j + B_j q + C_j q^2$ . See Appendix C.2 for how such values are computed. Using such formulation, we can solve a quadratic optimization problem, minimizing the maximum variance over  $\widehat{V}_q(f_j)$  over all possible values of  $q \in [0, 1/2]$  and for each  $j \in [k]$ . We first show that a sufficiently small bag of samples can yield a good estimate of the variance  $\widehat{V}_q(f_j)$ .

**LEMMA 3.13.** *There exist values  $A_j, B_j$ , and  $C_j$  obtained over  $c \geq 2$  sampled edges such that  $\mathbb{E}[\widehat{V}_q(f_j)] = \text{Var}[f_j]$  for*

$$\widehat{V}_q(f_j) = \frac{m^2}{(c-1)|V_j|^2} \left( \sum_{e \in \mathcal{S}} A_j + q B_j + C_j q^2 \right) .$$



The proof can be found in Appendix A.

The above lemma tells us that the estimates  $\widehat{V}_q(f_j)$  provide an unbiased approximation of the variance  $\text{Var}[f_j]$  for each function  $f_j$ . The next lemma tells us that such estimates are also a good approximation, for each value of  $q \in [0, 1/2]$ .

LEMMA 3.14. *There exist a small value  $\epsilon' > 0$  such that  $\widehat{V}_q(f_j) \in [\text{Var}[f_j] - \epsilon', \text{Var}[f_j] + \epsilon']$  for each partition  $j = 1, \dots, k$  and value of  $q \in [0, 1/2]$ , with high probability.*

The proof can be found in Appendix A.

To find the optimal value of  $q$ , given that we have a good estimate of  $\text{Var}[f_j]$ , for each  $j \in [k]$ , we solve the following convex problem, minimizing the largest estimated variance  $\widehat{V}_q(f_j)$  over  $j \in [k]$ .

PROBLEM 2 (OPTIMIZATION OF  $q$ ). *Let  $A_j, B_j$  and  $C_j$  be the coefficients contributing to estimate the variance  $\widehat{V}_q(f_j)$  then solving the following quadratic program yields  $x^* = q_{\text{alg}}$  such that  $\widehat{V}_{q_{\text{alg}}}(f_j) \in \widehat{V}_{q^*}(f_j) \pm \epsilon'$  for small  $\epsilon'$ , and controlled error probability, where  $q^*$  is the optimal value  $q$  minimizing the variance of functions  $f_j, j = 1, \dots, k$ .*

$$\begin{aligned} & \text{minimize} && t \\ & \text{subject to} && t \geq A_j + B_j x + C_j x^2, \text{ for all } j = 1, \dots, k, \\ & \text{and} && x \in [0, 1/2]. \end{aligned}$$

Solving this quadratic problem with state-of-the-art solvers is efficient:  $x$  is in  $\mathbb{R}$ , the sample size  $c$  used to compute the terms  $A_j, B_j, C_j$  in Algorithm 4 is a small constant, the objective function and the constraints are convex, and in practice  $k$  is small, yielding an overall efficient procedure (see Section 4.4). Note that in TRIAD we denote collectively with `Fixq` the procedure that computes both  $\widehat{V}_q(f_j)$ , for  $j \in [k]$ , and identifies  $x^* = q_{\text{alg}}$ .

3.3.4 UpperBounds. A detailed description of the UpperBounds subroutine, which requires linear time complexity in  $m$ , is reported in Appendix C.1.

The next lemma shows that UpperBounds outputs an upper bound on the ranges of  $f_j(e), e \in E$ , and  $\zeta$  as from Proposition 3.8.

LEMMA 3.15. *The output of UpperBounds is such that  $f_j(e) \leq R_j$  almost surely, for each  $e \in E$ , and partition  $V_j, j = 1, \dots, k$ , where  $\zeta$  corresponds to the pseudo-dimension bound from Proposition 3.8.*

### 3.4 Practical optimizations

In this section we introduce some practical optimizations to improve the performances of TRIAD, with minimal complexity overhead.

3.4.1 Improved empirical bounds. We can further refine the empirical bounds for terms  $\widehat{\epsilon}_j$ , for  $j \in [k]$  (in line 17) computed by TRIAD by leveraging the following result.

THEOREM 3.16 (PREDICTABLE PLUGIN-EMPIRICAL BERNSTEIN CONFIDENCE INTERVAL (PRPL-EB-CI) [52, 62]). *Let  $X_1, \dots, X_s$  be  $s$  i.i.d. random variables such that for all  $i = 1, \dots, s$ , it is  $\mathbb{E}[X_i] = \mu$  and*

$\mathbb{P}[X_i \in [a, b]] = 1$ , with  $R = |b - a|$ , and let

$$\begin{aligned} \omega(\lambda) &= \frac{-\log(1 - R\lambda) - R\lambda}{4} \text{ for } \lambda \in [0, 1/R], \quad \widehat{\mu}_j = \frac{1}{j} \sum_{i=1}^j X_i, \\ \widehat{\sigma}_j &= \frac{R^2/4 + \sum_{i=1}^j (X_i - \widehat{\mu}_{j-1})^2}{j}, \quad \lambda_{j,s} = \min \left\{ \sqrt{\frac{2 \log(2/\eta)}{s \widehat{\sigma}_{j-1}}}, \frac{1}{2R} \right\} \end{aligned}$$

for  $j = 1, \dots, s$ , where  $\widehat{\mu}_0 = 0$  and  $\widehat{\sigma}_0 = R^2/4$ . Then it holds that

$$\left| \frac{\sum_{i=1}^s \lambda_{i,s} X_i}{\sum_{i=1}^s \lambda_{i,s}} - \mu \right| \leq \frac{\log(2/\eta) + (2/R)^2 \sum_{i=1}^s [\omega(\lambda_{i,s})(X_i - \widehat{\mu}_{i-1})^2]}{\sum_{i=1}^s \lambda_{i,s}}$$

with probability at least  $1 - \eta$ .

While similar in spirit to Theorem 3.11, the above bound often yields a sharper empirical bound on the values  $\widehat{\epsilon}_j$ . Note that the above estimator yields a slightly more complicated formulation, i.e., the output of TRIAD corresponds to  $f_j = \frac{\sum_{i=1}^s \lambda_{i,s} f_j(e_i)}{\sum_{i=1}^s \lambda_{i,s}}$  where  $f_j(e_i)$  is the estimate associated to bucket  $V_j$ , for  $j \in [k]$  evaluated for the  $i$ -th sample from  $\mathcal{S}$ .

In addition, the stopping condition is evaluated using the bounds  $\frac{\log(2/\eta) + (2/R)^2 \sum_{i=1}^s [\omega(\lambda_{i,s})(X_i - \widehat{\mu}_{i-1})^2]}{\sum_{i=1}^s \lambda_{i,s}} = \widehat{\epsilon}_j \leq \epsilon_j$ , for  $j \in [k]$ , and  $f_j = \frac{1}{s} \sum f_j(e_i)$  if  $s \geq s_{\text{max}}$ . In Section 4, we leverage Theorem 3.16, but for ease of notation and presentation we introduced TRIAD with the results of Theorem 3.11.

3.4.2 Fixed sample size variant. In this section we briefly describe a variant that we call TRIAD-F, which leverages a fixed sample size schema. That is, in many applications, concentration bounds (e.g., Theorem 3.11), even if tight and empirical, can still be conservative. Hence we modify TRIAD to leverage the novel estimators discussed in Lemma 3.4, and the adaptive procedure to select the value of  $q$  as described in Section 3.3.3, but we modify the stopping condition of TRIAD. That is, we only require TRIAD-F to process at most a number  $s \geq 1$  samples as provided in input by the user. This is of interest in many applications where strictly sublinear time complexity is required. In fact, such modification strictly enforces a small number of samples to be processed. We show that such variant outputs highly accurate estimates of each bucket, by processing only 1% edges on most graphs (see Section 4.2).

3.4.3 Filtering very small degree-nodes. To enable better performance for TRIAD, we process the graph  $G$  by removing the nodes with small degree obtaining a graph  $G'$  where all the nodes' degrees, in  $G$ , are above a certain threshold. This step decreases the variance of the estimates computed by TRIAD, as small degree nodes can have high values for their metric  $\psi$  (i.e., close to 1), but sampling may perform poorly in approximating the values  $\psi$ , when computing the estimate  $f_j$ , for  $j \in [k]$ , similarly to what noted by de Lima et al. [15], Kutzkov and Pagh [27]. The key challenge is to bound the overall total work to  $\Theta(n)$  time complexity, making such processing negligible, and retaining the correct information to recover the solution to Problem 1 on  $G$ .

Our approach identifies a threshold over the node degree distribution, namely  $\beta$ , for which computing all the nodes' triangles under such threshold requires at most linear time in  $n$ , i.e., bounded by  $Cn$  for a small fixed constant  $C$ . Obtaining  $\Delta_v$  for a node  $v \in V$  with degree  $d_v$  requires at most  $O(d_v^2)$  time. Therefore we first identify

the value  $\beta$  such that  $\beta = \max_{i=1, \dots, d_{\max}} \beta_i$  such that  $\sum_{j=1}^i j^2 D_j \leq Cn$ , where  $D_i$  denotes the number of nodes in  $G$  such that their degree is exactly  $i$ , that is  $D_i = |\{v \in V : d_v = i\}|$ . Clearly,  $\beta$  can be computed in linear time  $\Theta(n)$  by iterating all nodes, assuming constant access to their degrees  $d_v$ . Given the threshold  $\beta$ , for each node  $v \in V$  with degree less than  $\beta$  we compute exactly the triangles  $\Delta_v$ , keeping track for all the nodes  $v \in V'$  that have degree higher than  $\beta$  of the triangles containing at least one removed node. We show that our approach is efficient and yields no additional estimation error for TRIAD in Appendix C.3.

### 3.5 Time and memory complexity

**Time complexity.** We recall that the filtering step requires  $O(n)$  total work, and the routine UpperBounds requires  $O(km)$ , while Fixq requires  $O(d_{\max} + T_{QP})$ . Note that  $T_{QP}$ , the complexity of solving the convex minimax problem, is negligible as the optimization is over  $k$  total convex non-integer constraints, and for our problem formulation we consider  $k$  as a (possibly large) constant.

Finally, the largest time complexity to perform the adaptive loop over  $T = s_{\max}$  total iterations of TRIAD, can require up to  $O(T(d_{\max} + T))$  time since: (1) each edge can be incident to  $d_{\max}$  nodes; (2) the additional  $T^2$  term is from computing the empirical variance at each iteration.<sup>7</sup> Hence the *worst case* complexity is  $O(R^2 \varepsilon^{-2} (\zeta + \log 1/\eta)(d_{\max} + T) + m)$ . Note that such analysis is extremely pessimistic, in fact, in practice the complexity of TRIAD is instead close to  $O(R \varepsilon^{-1} (\log k/\eta) d_{\max} + km)$ , as we often observe TRIAD to terminate after a small number of iterations of its main loop, implying that the processed edges are at most  $O(R \varepsilon^{-1} (\log k/\eta))$ . Hence, when  $O(R \varepsilon^{-1} (\log k/\eta))$  is a small fraction  $\omega \ll 1$  of  $m$  (e.g., 1% of  $m$ ) then the total complexity is bounded as  $O(m(d_{\max} \omega + k))$ , capturing the efficiency of TRIAD.

**Memory complexity.** The memory complexity of TRIAD is comparable to existing state-of-the-art methods [49] for estimating the local clustering coefficient, requiring  $O(m)$  memory. In more detail, TRIAD requires memory  $O(m + |S|k + kn)$ , where  $|S|$  is the size of the samples processed by TRIAD. Clearly  $|S| = s$  for TRIAD-F. When processing very large graphs with limited resources such complexity can be prohibitive, hence in such cases, we should rely on a (semi-)streaming or distributed (e.g., MPC) implementation of TRIAD [7, 25], an interesting future direction.

### 3.6 Adaptive guarantees

We briefly discuss the main advantages and limitations of TRIAD in the adaptive case. We observe that TRIAD has a significant advantage to solve Problem 1. Given an input graph  $G$  and a partition  $\mathcal{V}$ , TRIAD selects its estimators  $f_j$ , for  $j \in [k]$ , by properly fixing the parameter  $q$  *adaptively*. That is, the parameter  $q$  is optimized by TRIAD directly on  $G$ , leading to estimators  $f_j$ , for  $j \in [k]$ , with small variance as captured by our theoretical results in Lemma 3.14 and in practice in Section 4.2. TRIAD also adapts the number of processed samples ( $|S|$ ) by leveraging the results from Theorem 3.16. Such bounds involve the empirical variance  $\widehat{\sigma}_j$ , for  $j \in [k]$ , optimized by TRIAD through the parameter  $q$ —and the upper bounds  $R_j$  on the range of  $f_j(e)$ ,  $j \in [k]$ ,  $e \in E$ . Where each  $R_j$  depends on the node distribution over  $\mathcal{V}$  and  $G$ . Obtaining a non-trivial

<sup>7</sup>This complexity can be reduced to  $T$  by relying on the wimpy variance.

**Table 1: Datasets used in the experimental evaluation. Statistics show:  $n$  the number of nodes,  $m$  the number of edges,  $d_{\max}$  the maximum degree,  $\bar{\alpha}$  (resp.  $\bar{\phi}$ ) the average local clustering (resp. closure) coefficient over all nodes.**

Dataset	$n$	$m$	$d_{\max}$	$\bar{\alpha}$	$\bar{\phi}$
fb-CMU	6.6 <i>K</i>	0.3 <i>M</i>	$8 \cdot 10^2$	0.27	0.12
SP	1.6 <i>M</i>	22 <i>M</i>	$1 \cdot 10^4$	0.11	0.03
FR	12 <i>M</i>	72 <i>M</i>	$3 \cdot 10^3$	0.08	0.01
OR	3.1 <i>M</i>	0.1 <i>B</i>	$3 \cdot 10^4$	0.17	0.06
LJ	4.8 <i>M</i>	43 <i>M</i>	$2 \cdot 10^4$	0.27	0.08
BM	43 <i>K</i>	14 <i>M</i>	$8 \cdot 10^3$	0.51	0.19
G500	4.6 <i>M</i>	0.1 <i>B</i>	$3 \cdot 10^5$	0.06	0.0
GP	0.1 <i>M</i>	12 <i>M</i>	$2 \cdot 10^4$	0.49	0.05
PT	43 <i>K</i>	44 <i>K</i>	$2 \cdot 10^1$	0.12	0.1
HW	1.1 <i>M</i>	56 <i>M</i>	$1 \cdot 10^4$	0.77	0.16
HG	0.5 <i>M</i>	13 <i>M</i>	$5 \cdot 10^4$	0.19	0.01
BNH	0, 7 <i>M</i>	0.2 <i>B</i>	$2 \cdot 10^4$	0.5	0.3
TW	0.2 <i>M</i>	6.8 <i>M</i>	$4 \cdot 10^4$	0.16	0.01

characterization of  $R_j$  is extremely challenging, but we observe the following. When the values  $R_j$  are large in practice the obtained empirical bounds  $\widehat{\varepsilon}_j$  may be loose with respect to the actual deviations  $|f_j - \Psi_j|$ . Instead, when  $R_j \in O(1)$  then TRIAD processes  $\widetilde{O}(1/\varepsilon)$  samples (a significant improvement over  $\widetilde{O}(1/\varepsilon^2)$ ).<sup>8</sup> This is an inherent trade-off, when  $R \in O(1)$  then the runtime of TRIAD is almost constant providing tight bounds  $\widehat{\varepsilon}_j \leq |f_i - \Psi_i|$ , which depend on  $G$  and  $\mathcal{V}$ .

## 4 EXPERIMENTAL EVALUATION

In this section we present our extensive experimental evaluation. We start by first describing the setup, and then we discuss the results of our research questions.

### 4.1 Setting

**Implementation details.** We implemented our algorithms in C++20, and compiled it under gcc 9.4, with optimization flags. To solve the variance optimization problem (Section 3.3.3) we used Gurobi 11 under academic license. All the experiments were performed on a 72-core machine Intel Xeon Gold, running Ubuntu 20.04. The code to reproduce our results is publicly available.<sup>9</sup>

**Datasets and partitions into buckets.** For our experiments we consider multiple datasets available online, from medium to large sized, which are reported together with a summary of their statistics in Table 1. More details on such datasets, are in Appendix F.1.1.

For each dataset we considered three main different node partitions  $\mathcal{V}$ : (i)  $\mathcal{V}_{core}$  is obtained by grouping nodes with similar core-number over a total of  $k = 30$  buckets; (ii)  $\mathcal{V}_{deg}$  is obtained by grouping together nodes with similar degrees over a total of  $k = 25$  buckets; (iii)  $\mathcal{V}_{logDeg}$  assigns each node to a bucket as function of its degree [25], i.e., a node with degree  $d$  is assigned to the bucket with index  $\lfloor \log(1 + (d - 2)/\log 2) \rfloor + 2$ , hence it holds  $k = O(\log n)$ .

<sup>8</sup>In  $\widetilde{O}(\cdot)$  we ignore logarithmic factors.

<sup>9</sup><https://github.com/iliesarpe/Triad>.



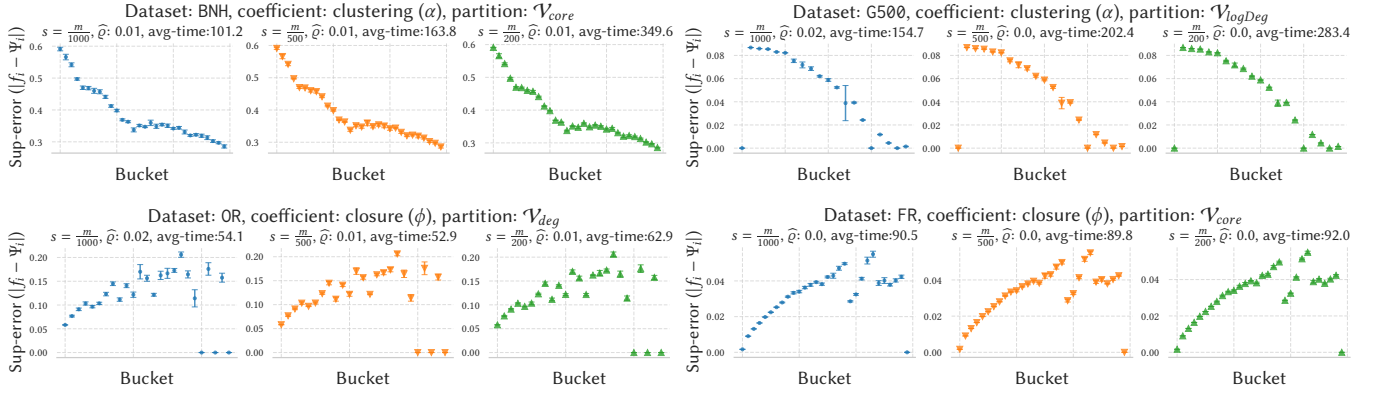


**Figure 3: Value  $\Psi_i$  and its maximum error ( $|f_i - \Psi_i|$ ) over five runs. We also report, the supremum error  $\hat{q} = \sup_{i \in [k]} |f_i - \Psi_i|$  and the average runtime over five independent runs across all buckets, for varying sample size ( $s \in \{1, 2, 5\}\%$  of the total edges  $m$ ).**

Note that all the above partition schemes place nodes with similar degree in the same bucket. This is often the case in practical applications, where nodes with similar degree are associated to similar structural functions [25].

In addition, To test a general input to Problem 1 we also consider two other partitions  $\mathcal{V}$ . Partition  $\mathcal{V}_{rnd}$  assigns nodes at random into  $k = 30$  buckets and  $\mathcal{V}_{met}$  is obtained by clustering with  $k = 10$  each graph using METIS [24]. We report the results obtained on these partitions in Appendix F.2 as they follow similar trends to the ones discussed below. We do not discuss the memory usage as it is similar to all algorithms (TRIAD uses slightly more space compared to baselines as from our analysis in Section 3.5).

Finally we use TRIAD- $\alpha$  (resp. TRIAD- $\phi$ ) to denote TRIAD when used to approximate the average local clustering (resp. local closure) coefficient.

**Research questions.** Our experimental evaluation investigated the following research questions.

- Q1.** How TRIAD performs in terms of accuracy and efficiency when varying its sample size  $s$ ? (Section 4.2)
- Q2.** How tight are the adaptive guarantees provided by TRIAD, compared to state-of-the-art approaches? (Section 4.3)
- Q3.** What is the runtime of TRIAD; what is the impact of parameter  $q$ , and what is the quality of our optimization of  $q$ ? (Section 4.4)
- Q4.** Which patterns are captured by triadic coefficients and TRIAD over collaboration networks? (Section 4.5)

## 4.2 Accuracy of estimates and efficiency

In this section we answer **Q1**, i.e., we study TRIAD’s accuracy and efficiency by varying the sample size  $s$ . This setting is fundamental to show that TRIAD is both efficient and provides extremely accurate estimates by processing a small number of edges.

**Setting.** We consider TRIAD-F, which retains the adaptive selection of the parameter  $q$  while terminating TRIAD’s main loop after processing exactly  $s$  samples (see Section 3.4.2). To set  $s$  we considered three different values:  $s = 1\%$ ,  $s = 2\%$ , and  $s = 5\%$  of the total edges  $m$  of each dataset. We then run each configuration (dataset,

value of  $s$ , and bucket partition) for five independent runs. We then measure for each bucket the supremum error  $|f_i - \Psi_i|$  over the five runs, and  $\hat{q}$  the supremum of such errors across all buckets of  $\mathcal{V}$ . In addition, we measure the average runtime to process  $s$  samples over the five runs. Some representative results are presented in Figure 3.

**Results.** First, over almost all configurations tested we note that TRIAD’s estimates are very accurate and tightly concentrated for each bucket of the various partitions. This is reflected by the supremum error  $\hat{q}$ , which is small and almost negligible even for very small sample sizes  $s$  such as  $s=1\%$ . This holds in particular for datasets BNH and FR, while TRIAD requires a slightly higher sample size (i.e.,  $s=2\%$ ) to provide extremely accurate estimates for datasets G500 and OR. Note that the supremum error with a sample size of  $s=2\% \cdot m$  tends to 0 on the considered configurations on all datasets. This supports the fact that TRIAD requires only a very small number of samples to obtain highly accurate estimates for Problem 1.

In addition, TRIAD’s runtime is limited by at most a few hundred of seconds on very large datasets, yielding estimates almost comparable to the exact unknown values, showing that TRIAD is both efficient and highly accurate on both triadic coefficients. Further results are presented in Appendix F.2

**Summary.** A very small sample size (of  $1\%$  total edges) is often sufficient to obtain highly accurate estimates for TRIAD, *simultaneously* over all buckets and different partitions for both the average local triadic coefficients, which is remarkable and extremely useful for highly-scalable network analysis.

## 4.3 Comparison with state-of-the-art

In this section we address **Q2**, i.e., we evaluate TRIAD and its adaptive guarantees with respect to existing state-of-the-art approaches.

**Setting.** We consider the state-of-the-art approach to approximate the local clustering coefficient values [49] (see Section 5), denoted with WedgeSampler- $\alpha$  (or WS- $\alpha$  for short). We extend the idea of wedge sampling to approximate the local closure coefficient, as there are no algorithms tailored for the local closure coefficient. This baseline, denoted with WedgeSampler- $\phi$ , is detailed in Appendix D. We fix  $\varepsilon_j = \varepsilon = 0.075$  for all datasets and all buckets in  $\mathcal{V}$

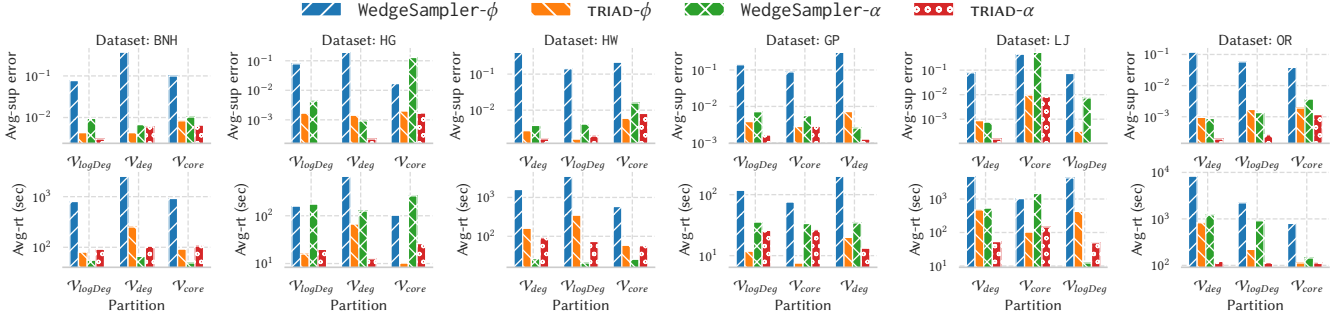


**Figure 4: Comparison of TRIAD and the baselines WedgeSampler.** For each dataset we show, (top plot): the average supremum error over all buckets over the various runs. (bottom): average runtime to perform an execution.



**Figure 5: Fine grained runtime analysis.** We show the average fraction of time spent in each step by TRIAD, the setting is from Section 4.3.

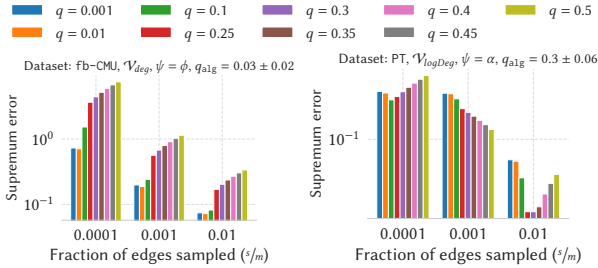


**Figure 6: Supremum error over ten runs over different partitions, sample size  $s$ , coefficient  $\psi$ , and values of  $q$ .**

for TRIAD and  $\eta = 0.01$ , additional parameters are reported in Appendix F.1.2. For each configuration we run TRIAD and obtain  $\hat{\epsilon}_j$ , i.e., the adaptive upper bounds on the distance between the estimates  $f_j$  and the unknown values  $\Psi_j$  for each bucket  $V_j \in \mathcal{V}$ . We then use such values as input for WedgeSampler, such that both algorithms provide the same guarantees. For each configuration we compute the estimation error as the supremum error  $|f_j - \Psi_j|$ , averaged over all buckets, our results will show the maximum of such supremum error over five runs. In addition, we report the average runtime for each algorithm on the various configurations, which was time-limited for all algorithms.

**Results.** Key results are summarized in Figure 4. We first observe that TRIAD reports very accurate estimates for  $\Psi_j$  on most configurations, which are much more precise than the ones provided by WedgeSampler. In particular, the supremum error, as desired, is of the order of  $10^{-2}$  and on some configurations up to  $10^{-3}$  (e.g., for datasets HG and OR). The baselines on most configurations achieve higher errors than TRIAD. We observe that this is especially the case for WedgeSampler- $\phi$  achieving higher error than TRIAD. Importantly, we observe that the range of improvement in accuracy over the baseline is up to one order of magnitude.

Remarkably, such results are obtained with a comparable or significantly smaller runtime with respect to the state-of-the-art baseline WedgeSampler (up to one order of magnitude on datasets HG, LJ and OR). In fact, our experiments confirm that TRIAD provides tighter bounds on the deviation between its estimates ( $f_j$ ) and the unknown values ( $\Psi_j$ ), significantly better than existing approaches, while being more efficient. Unfortunately, in practice, such bounds may still be loose—this can be noted by observing that we provided in input to TRIAD  $\epsilon_j = 0.075$  and under various datasets (e.g., HG, OR and LJ) the maximum errors for TRIAD are much smaller.

**Summary.** Our algorithm TRIAD provides better bounds on the deviation between the estimates  $f_j$  and the unknown coefficients  $\Psi_j$ , compared to existing approaches. While being tighter, such guarantees may still be loose for some settings, leaving an open question for future directions.

## 4.4 Runtime and parameter sensitivity

**4.4.1 Runtime analysis.** In this section we analyze TRIAD’s runtime. In particular, we split the runtime into the following steps: (i) the practical optimization over the small-degree nodes; (ii) the optimization of the variance through Fixq; (iii) the execution of the routine UpperBounds; and (iv) the adaptive loop.

Figure 5 reports the average fraction of time spent by TRIAD in the various steps over the experiments from Section 4.3. We report two very different behaviors. On dataset OR, except for  $V_{deg}$ , the time of performing the adaptive loop is negligible compared with all the other steps. This is in contrast with dataset GP, where most of TRIAD’s runtime is spent in its adaptive loop, highlighting that TRIAD effectively adapts to the complexity of the graph in input. In other words, when the variance of the coefficients  $\psi_v$  is

small, then the adaptive loop can terminate by processing a small amount of samples  $s$  as captured by Theorem 3.16.

Interestingly, we note that the procedure to optimize the variance (that we denote with  $\text{Fix}q$ ) is often negligible, especially compared with  $\text{UpperBounds}$ , as captured by our analysis in Section 3.3.3.

Our results show that TRIAD’s runtime depends on the complexity of the input graph i.e., the distribution of the unknown coefficients across buckets in  $\mathcal{V}$ , which allows TRIAD to compute highly accurate estimates very efficiently through its adaptive bounds.

**4.4.2 Assessing the impact of  $q$ .** In this section we investigate the impact of the parameter  $q$  on the quality of the estimates computed by TRIAD. Recall that  $q$  controls how the estimates  $f_j$  are computed, affecting the variance of the results. To evaluate such parameter, we selected two of our smallest datasets, for computational efficiency, and a fixed grid of nine values for the parameter  $q$ . For each value of  $q$  we then tested different sample sizes, i.e., using TRIAD-F with a sample size  $s$  such that  $s/m \in \{0.0001, 0.001, 0.01\}$ . For each combination of dataset, partition  $\mathcal{V}$ , value of  $q$ , and sample size  $s$ , we performed ten runs over both triadic coefficients  $\psi \in \{\phi, \alpha\}$ .

Some representative results are shown in Figure 6 reporting the supremum error (i.e.,  $\sup_j |f_j - \Psi_j|$ ) over the various configurations. We observe that the impact of  $q$  on the estimates  $f_j$ , over all sample sizes, can be from negligible (on the bottom-left plot) to very significant (bottom-right plot). In general, we observe a significant reduction in the supremum error by a proper selection of the value of  $q$ —up to one order of magnitude in several settings (such as the top-left or bottom-right plots). This behavior confirms the importance of properly selecting the value of  $q$ . We note that the supremum error tends to be minimized with a specific value of  $q$  over the different settings, but this value is, in general, different on most configurations (e.g., top- and bottom-right plots).

Summarizing, a proper selection of the value of  $q$  can have a significant impact on the estimates of TRIAD leading to up to one order of accuracy in the estimates. The next section assesses how well our optimization aligns with a good value of the parameter  $q$ .

**4.4.3 Optimization of  $q$ .** We now briefly assess how well the value of  $q_{\text{alg}}$  (as optimized by TRIAD) aligns with a good choice for the parameter  $q$ . Results are shown in Figure 6, where we report the average  $q_{\text{alg}}$  and its standard deviation over ten runs. The size of the bag of samples used to compute  $q_{\text{alg}}$  is set to 500.

As captured by our analysis, the value of  $q_{\text{alg}}$  well-aligns with a good value of  $q$  obtained from the grid of tested values, on each configuration. In fact,  $q_{\text{alg}}$  often overlaps with the  $q$  yielding the minimum supremum error from the grid. For example, on the top-left plot the best value on the grid is  $q = 0.01$  while  $q_{\text{alg}} = 0.03 \pm 0.02$ , highlighting that our method properly selects a good value for  $q$ , yielding small estimation variance.

## 4.5 Case study—academic collaborations

In this section we analyze collaboration patterns in different communities of the DBLP network using TRIAD, answering Q4.

**Setting.** DBLP collects bibliographic information about all major computer science journals and proceedings publications.<sup>10</sup> For each time-period of five consecutive years from 1970 to 2024, we collected

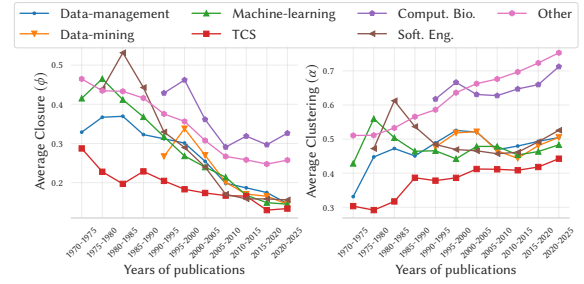


**Figure 7: Average local clustering and local closure coefficient over the DBLP graph snapshots, for various computer science communities.**

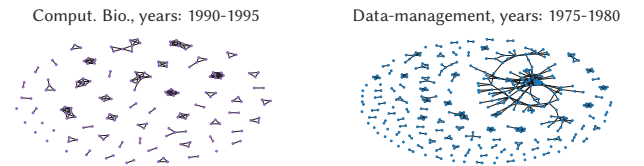


**Figure 8: Induced subgraphs by communities. (Left): computational biology; (Right): data-management.**

the respective set of publications over DBLP. On each time period  $t_1 = [1970, 1975]$ ,  $t_2 = [1975, 1980]$ , ... we build a graph  $G_{t_i} = (V_{t_i}, E_{t_i})$ , with  $V_{t_i}$  consisting of authors, and edges corresponding to authors sharing a common publication. We then classified the authors, on each graph  $G_{t_i}$ , according to their research community. The resulting categories are reported in the legend of Figure 7, additional details on the classification are in Appendix F.1.3.

For each graph we computed the average triadic coefficients over each category. We then investigated if the analysis of the coefficients  $f_j$ , for  $j \in [k]$ , provides us insights into similarities and differences of collaboration patterns over different communities.

**Results.** We observe in Figure 7 some interesting trends. For most of the communities, the average local clustering coefficient increases or remains stable over the years. Instead, the average local closure coefficient mostly decreases, for all but the computational-biology community. This can be explained by the fact that, new nodes over the network, are likely to have a small local closure coefficient when they collaborate with an author having many coauthors (e.g., students publishing with their advisor). Instead, it is easier for novel nodes on the network to have higher local clustering coefficient, e.g., by collaborations within research groups. In addition, it is also easier for authors already belonging to the network to increase their local clustering coefficient over time, e.g., by publishing more.

There is a, perhaps surprising, increase in the average local closure coefficient for the computational-biology community over time. This could be explained by the fact that publications in this area require the joint effort of many authors, which likely increases the density of the connections of the authors in the graphs. Such an aspect can be observed in Figure 8, where we see that the structure of collaborations over the computational biology category forms

<sup>10</sup><https://dblp.org/>

**Table 2: Comparison of TRIAD and existing state-of-the-art approaches.**  $\Psi$ : if the algorithm can estimate  $\alpha$ ,  $\phi$ , or both. “Adaptive” denotes if the estimates adapt to the partitions  $\mathcal{V}$ . “Number of samples” denotes the number of samples processed. Finally “Processing complexity” denotes the time to process a sample, assuming  $O(1)$  time complexity to check the existence of an edge. For ThinkD,  $r$  denotes the number of retained edges, which depends on  $\varepsilon^{-2}$ .

Algorithm	$\Psi$	Adaptive	Number of samples	Processing complexity
TRIAD	$\alpha, \phi$	✓	$\Omega\left(\frac{R \log k / \eta}{\varepsilon}\right)$ and $O\left(R^2 \frac{\zeta + \log 1/\eta}{\varepsilon^2}\right)$	$O(d_{\max})$
WS- $\alpha$ [49]	$\alpha$	✗	$\Theta(k\varepsilon^{-2} \log k / \eta)$	$O(1)$
WS- $\phi$	$\phi$	✗	$\Theta(k\varepsilon^{-2} \log k / \eta)$	$O(d_{\max})$
LCE [15]	$\alpha$	✗	$\Theta(m^2 \varepsilon^{-2} (\log d_{\max} + \log 1/\eta))$	$O(d_{\max})$
ECC [27]	$\alpha$	✗	$O(\varepsilon^{-2} \log n / \eta)$	$O(m \log \varepsilon^{-1})$
ThinkD [55]	$\alpha$	✗	$O(r)$	$\Theta(m)$

many cliques. On the other hand, the structure of the graph of the data management community is more sparse, containing some chain structures. We further visualize the subgraph of other categories in Appendix F.4. We conclude by noting that the average local clustering coefficient is significantly higher (ranging from 0.4 to more than 0.6) than the average local closure coefficient (which does not exceed 0.35) over all communities. This may be related to the nature of academic collaborations, where publishing with established researchers decreases the local closure coefficient of novel researchers on average. We further discuss that the above results cannot be uniquely explained by the degree distribution of the various nodes, in Appendix F.4.

**Summary.** We analyzed the average local clustering (and closure) coefficients over different computer science communities across time. We observed that the values of the triadic coefficient can capture different collaboration patterns. For example, capturing highly collaborative (computational biology) and more sparse (data management) communities. Our findings show an example of a simple analysis using Problem 1 to gain better insights into publication and collaboration patterns in different research communities.

## 5 RELATED WORK

The problems addressed in this paper are closely related to counting triangles in graphs, which has been studied extensively. Thus, an extensive review is outside the scope [3, 50], instead, we focus only on discussing the most relevant problem settings and techniques.

**Clustering and closure coefficient algorithms.** The local clustering coefficient was first introduced by Watts and Strogatz [61]. Since their seminal work, many algorithms have been developed to efficiently compute related graph statistics. Many approaches consider both the approximation of the global clustering coefficient [12, 48], which is the local clustering coefficient averaged over all nodes in the graph, and the transitivity coefficient, which is the fraction of closed triangles over all the wedges in the graph [17], or weighted versions [28]. Interestingly, TRIAD can be adapted to compute all those coefficients with minimal modifications.

Many algorithms have been designed for computing the local clustering coefficient in restricted access models, such as (i) when

the graph can be explored only through random walks [19]; (ii) when the graph is accessed in a (semi-)streaming fashion [7, 27]; or (iii) distributed environments [25]. Given that these works focus on restrictive scenarios, they require a large number of samples and often do not offer accurate guarantees.

The works most related to our formulation are by Etemadi and Lu [17], and Seshadhri et al. [49] who developed wedge-sampling algorithms, which, for each partition, sample wedges (i.e., our baseline considered in Section 4.3). These algorithms require a significantly high sample size, i.e.,  $\Theta(k\varepsilon^{-2} \log(k/\eta))$ , which is tight [6]. Therefore these algorithms become impractical for small values of  $\varepsilon$ , as also demonstrated in our experiments.

Recently, de Lima et al. [15] developed an algorithm based on sampling edges and collecting their incident triangles, to approximate the local clustering coefficient of nodes with high-degree. The authors prove an upper bound on the sample complexity using VC-dimension. While their approach is similar in spirit to ours, it is significantly less general, i.e., their approach can be obtained by our class of estimators setting  $q = 0$  in Equation (1). Their approach is also significantly less efficient, as their algorithm is based on data-independent bounds. In addition, our bound, as captured by Corollary 3.9, is significantly tighter than theirs.

Surprisingly, not much work has been done on algorithms for the closure coefficient. Recent works only quantify how this coefficient evolves in random networks [68].

**Triangle-counting algorithms.** As already noted, triangle counting is a wide area of research [4, 16, 26, 31, 58]. Most existing works address the problem of computing *global* triangle counts, and cannot therefore be used in our setting. Several works have been instead developed for *local* triangle counting. Exact methods [31, 39] are prohibitive for large networks, and sampling methods are designed for streaming settings [1, 54–56]. Those algorithms can provide accurate estimates for the local clustering coefficient when nodes have very high degree, while they are highly inaccurate for nodes with small degree. Note that this is a significant limitation for the setting we consider in this paper, where partitions may contain a large number of nodes with small degree.

**Subgraph-counting algorithms.** Another related problem is the one of counting subgraph occurrences, for which many different methods have been proposed [11, 20, 31, 42, 46, 47]. While these algorithms can be effectively used to count subgraph occurrences with respect to specific or multiple subgraph patterns, they cannot be easily adapted to extract high-quality local subgraph counts and average local triadic coefficients, as considered in Problem 1. Finally, Ahmed et al. [2] develop methods to estimate local subgraph counts, but compute *exactly* all triangles in the graph. A summary of the key differences with most related works is reported in Table 2. Note that the last two algorithms are for streaming settings [27, 55], hence we did not consider them in Section 4, as they are designed for a more restrictive data-access model, yielding more inefficient methods. We observe from Table 2 that depending on the evaluation of the adaptive bounds on the given datasets TRIAD can be highly efficient (i.e., when  $R$  is small), improving significantly over existing methods as shown in Section 4.

## 6 CONCLUSION

We studied the problem of efficiently computing the average of local triadic coefficients. We designed TRIAD, an efficient and adaptive sampling algorithm. TRIAD estimates both the average local clustering coefficient and the recently-introduced average local closure coefficient, for which no algorithmic techniques were previously known. We showed that TRIAD is efficient and reports extremely accurate estimates, especially compared with existing methods.

There are several interesting directions for future work, such as considering TRIAD for averages of local coefficients, which depend on the given partitions (e.g., a triangle is weighted differently if it contains nodes from different buckets), and weighted variants of the clustering and closure coefficients [28]. Another interesting direction is to adapt TRIAD for a multi-pass streaming setting [7, 27]. Finally, it will be interesting to study whether it is possible to design tighter bounds on the sample complexity, e.g., based on Rademacher complexity [40, 41].

## ACKNOWLEDGMENTS

We thank Fabio Vandin for providing us the computing infrastructure. This research is supported by the ERC Advanced Grant REBOUND (834862), the EC H2020 RIA project SoBigData++ (871042), and the Wallenberg AI, Autonomous Systems and Software Program (WASP) funded by the Knut and Alice Wallenberg Foundation.

## REFERENCES

- [1] Nesreen K. Ahmed, Nick Duffield, Theodore L. Willke, and Ryan A. Rossi. 2017. On sampling from massive graph streams. *Proceedings of the VLDB Endowment* 10, 11 (Aug. 2017), 1430–1441. <https://doi.org/10.14778/3137628.3137651>
- [2] Nesreen K. Ahmed, Theodore L. Willke, and Ryan A. Rossi. 2016. Estimation of local subgraph counts. In *2016 IEEE International Conference on Big Data (Big Data)*. IEEE. <https://doi.org/10.1109/bigdata.2016.7840651>
- [3] Mohammad Al Hasan and Vachik S. Dave. 2017. Triangle counting in large networks: a review. *WIREs Data Mining and Knowledge Discovery* 8, 2 (Oct. 2017). <https://doi.org/10.1002/widm.1226>
- [4] David A. Bader. 2023. Fast Triangle Counting. In *2023 IEEE High Performance Extreme Computing Conference (HPEC)*. IEEE, 1–6. <https://doi.org/10.1109/hpec58863.2023.10363539>
- [5] David A. Bader, Fuhuan Li, Zhihui Du, Palina Pauliuchenka, Oliver Alvarado Rodriguez, Anant Gupta, Sai Sri Vastav Minnal, Valmik Nahata, Anya Ganeshan, Ahmet Gundogdu, and Jason Lew. 2024. Cover Edge-Based Novel Triangle Counting. <https://doi.org/10.48550/ARXIV.2403.02997>
- [6] Thomas Baignères, Pascal Junod, and Serge Vaudenay. 2004. *How Far Can We Go Beyond Linear Cryptanalysis?* Springer Berlin Heidelberg, 432–450. [https://doi.org/10.1007/978-3-540-30539-2\\_31](https://doi.org/10.1007/978-3-540-30539-2_31)
- [7] Luca Becchetti, Paolo Boldi, Carlos Castillo, and Aristides Gionis. 2010. Efficient algorithms for large-scale local triangle counting. *ACM Transactions on Knowledge Discovery from Data* 4, 3 (oct 2010), 1–28. <https://doi.org/10.1145/1839490.1839494>
- [8] Sourav S. Bhowmick and Boon Siew Seah. 2016. Clustering and Summarizing Protein-Protein Interaction Networks: A Survey. *IEEE Transactions on Knowledge and Data Engineering* 28, 3 (March 2016), 638–658. <https://doi.org/10.1109/tkde.2015.2492559>
- [9] Filippo Maria Bianchi, Daniele Grattarola, and Cesare Alippi. 2019. Spectral Clustering with Graph Neural Networks for Graph Pooling. <https://doi.org/10.48550/ARXIV.1907.00481>
- [10] Michele Borassi and Emanuele Natale. 2019. KADABRA is an Adaptive Algorithm for Betweenness via Random Approximation. *ACM Journal of Experimental Algorithmics* 24 (Feb. 2019), 1–35. <https://doi.org/10.1145/3284359>
- [11] Marco Bressan, Stefano Leucci, and Alessandro Panconesi. 2019. Motivo: fast motif counting via succinct color coding and adaptive sampling. *Proceedings of the VLDB Endowment* 12, 11 (July 2019), 1651–1663. <https://doi.org/10.14778/3342263.3342640>
- [12] Luciana S. Buriol, Gereon Frahling, Stefano Leonardi, and Christian Sohler. [n.d.]. *Estimating Clustering Indexes in Data Streams*. Springer Berlin Heidelberg, 618–632. [https://doi.org/10.1007/978-3-540-75520-3\\_55](https://doi.org/10.1007/978-3-540-75520-3_55)
- [13] Norishige Chiba and Takao Nishizeki. 1985. Arboricity and Subgraph Listing Algorithms. *SIAM J. Comput.* 14, 1 (feb 1985), 210–223. <https://doi.org/10.1137/0214017>
- [14] Marek Ciglan, Alex Averbuch, and Ladi Lav Hluchy. 2012. Benchmarking Traversal Operations over Graph Databases. In *2012 IEEE 28th International Conference on Data Engineering Workshops*. IEEE, 186–189. <https://doi.org/10.1109/icdew.2012.47>
- [15] Alane M. de Lima, Murilo V. G. da Silva, and André L. Vignatti. 2022. *Estimating the Clustering Coefficient Using Sample Complexity Analysis*. Springer International Publishing, 328–341. [https://doi.org/10.1007/978-3-031-20624-5\\_20](https://doi.org/10.1007/978-3-031-20624-5_20)
- [16] Talya Eden, Amit Levi, Dana Ron, and C. Seshadhri. 2017. Approximately Counting Triangles in Sublinear Time. *SIAM J. Comput.* 46, 5 (Jan. 2017), 1603–1646. <https://doi.org/10.1137/15m1054389>
- [17] Roohollah Etemadi and Jianguo Lu. 2017. Bias correction in clustering coefficient estimation. In *2017 IEEE International Conference on Big Data (Big Data)*. IEEE, 606–615. <https://doi.org/10.1109/bigdata.2017.8257976>
- [18] Yixiang Fang, Xin Huang, Lu Qin, Ying Zhang, Wenjie Zhang, Reynold Cheng, and Xuemin Lin. 2019. A survey of community search over big graphs. *The VLDB Journal* 29, 1 (July 2019), 353–392. <https://doi.org/10.1007/s00778-019-00556-x>
- [19] Stephen J. Hardiman and Liran Katzir. 2013. Estimating clustering coefficients and size of social networks via random walk. In *Proceedings of the 22nd international conference on World Wide Web (WWW '13)*. ACM, 539–550. <https://doi.org/10.1145/2488388.2488436>
- [20] Madhav Jha, C. Seshadhri, and Ali Pinar. 2015. Path Sampling. In *Proceedings of the 24th International Conference on World Wide Web*. International World Wide Web Conferences Steering Committee. <https://doi.org/10.1145/2736277.2741101>
- [21] Bin Jiang, Sijian Zhao, and Junjun Yin. 2008. Self-organized natural roads for predicting traffic flow: a sensitivity study. *Journal of Statistical Mechanics: Theory and Experiment* 2008, 07 (July 2008), P07008. <https://doi.org/10.1088/1742-5468/2008/07/p07008>
- [22] Ruoming Jin, Victor E. Lee, and Hui Hong. 2011. Axiomatic ranking of network role similarity. In *Proceedings of the 17th ACM SIGKDD international conference on Knowledge discovery and data mining (KDD '11)*. ACM, 922–930. <https://doi.org/10.1145/2020408.2020561>
- [23] Marcus Kaiser. 2008. Mean clustering coefficients: the role of isolated nodes and leafs on clustering measures for small-world networks. *New Journal of Physics* 10, 8 (Aug. 2008), 083042. <https://doi.org/10.1088/1367-2630/10/8/083042>
- [24] George Karypis and Vipin Kumar. 1998. A Fast and High Quality Multilevel Scheme for Partitioning Irregular Graphs. *SIAM Journal on Scientific Computing* 20, 1 (Jan. 1998), 359–392. <https://doi.org/10.1137/s1064827595287997>
- [25] Tamara G. Kolda, Ali Pinar, Todd Plantenga, C. Seshadhri, and Christine Task. 2014. Counting Triangles in Massive Graphs with MapReduce. *SIAM Journal on Scientific Computing* 36, 5 (jan 2014), S48–S77. <https://doi.org/10.1137/13090729x>
- [26] Mihail N. Kolountzakis, Gary L. Miller, Richard Peng, and Charalampos E. Tsourakakis. 2012. Efficient Triangle Counting in Large Graphs via Degree-Based Vertex Partitioning. *Internet Mathematics* 8, 1-2 (mar 2012), 161–185. <https://doi.org/10.1080/15427951.2012.625260>
- [27] Konstantin Kutzkov and Rasmus Pagh. 2013. On the streaming complexity of computing local clustering coefficients. In *Proceedings of the sixth ACM international conference on Web search and data mining (WSDM 2013)*, Vol. 5. ACM, 677–686. <https://doi.org/10.1145/2433396.2433480>
- [28] Silvio Lattanzi and Stefano Leonardi. 2016. Efficient computation of the Weighted Clustering Coefficient. *Internet Mathematics* 12, 6 (June 2016), 381–401. <https://doi.org/10.1080/15427951.2016.1198281>
- [29] Jure Leskovec, Ajit Singh, and Jon Kleinberg. 2006. *Patterns of Influence in a Recommendation Network*. Springer Berlin Heidelberg, 380–389. [https://doi.org/10.1007/11731139\\_44](https://doi.org/10.1007/11731139_44)
- [30] Jure Leskovec and Rok Sosič. 2016. SNAP: A General-Purpose Network Analysis and Graph-Mining Library. *ACM Transactions on Intelligent Systems and Technology* 8, 1 (July 2016), 1–20. <https://doi.org/10.1145/2898361>
- [31] Qiyan Li and Jeffrey Xu Yu. 2024. Fast Local Subgraph Counting. *Proceedings of the VLDB Endowment* 17, 8 (April 2024), 1967–1980. <https://doi.org/10.14778/3659437.3659451>
- [32] Rong-Hua Li, Lu Qin, Jeffrey Xu Yu, and Rui Mao. 2015. Influential community search in large networks. *Proceedings of the VLDB Endowment* 8, 5 (Jan. 2015), 509–520. <https://doi.org/10.14778/2735479.2735484>
- [33] Yusheng Li, Yilun Shang, and Yiting Yang. 2017. Clustering coefficients of large networks. *Information Sciences* 382–383 (March 2017), 350–358. <https://doi.org/10.1016/j.ins.2016.12.027>
- [34] Andreas Maurer and Massimiliano Pontil. 2009. Empirical Bernstein Bounds and Sample Variance Penalization. (July 2009). <https://doi.org/10.48550/ARXIV.0907.3740> arXiv:0907.3740 [stat.ML]
- [35] Michael Mitzenmacher. 2017. *Probability and computing* (second edition ed.). Cambridge University Press, Cambridge. Hier auch später erschienene, unveränderte Nachdrucke.
- [36] Volodymyr Mnih, Csaba Szepesvári, and Jean-Yves Audibert. 2008. Empirical Bernstein stopping. In *Proceedings of the 25th international conference on Machine learning - ICML '08 (ICML '08)*. ACM Press, 672–679. <https://doi.org/10.1145/1390156.1390241>
- [37] Mark Newman. 2018. *Networks*. Oxford University Press. <https://doi.org/10.1093/oso/9780198805090.001.0001>



- [38] Xiaohui Pan, Guiqiong Xu, Bing Wang, and Tao Zhang. 2019. A Novel Community Detection Algorithm Based on Local Similarity of Clustering Coefficient in Social Networks. *IEEE Access* 7 (2019), 121586–121598. <https://doi.org/10.1109/access.2019.2937580>
- [39] Noujan Pashanasangi and C. Seshadhri. 2020. Efficiently Counting Vertex Orbits of All 5-vertex Subgraphs, by EVOKE. In *Proceedings of the 13th International Conference on Web Search and Data Mining (WSDM '20)*. ACM. <https://doi.org/10.1145/3336191.3371773>
- [40] Leonardo Pellegrina. 2023. Efficient Centrality Maximization with Rademacher Averages. In *Proceedings of the 29th ACM SIGKDD Conference on Knowledge Discovery and Data Mining*. ACM. <https://doi.org/10.1145/3580305.3599325>
- [41] Leonardo Pellegrina and Fabio Vandin. 2023. SILVAN: Estimating Betweenness Centralities with Progressive Sampling and Non-uniform Rademacher Bounds. *ACM Transactions on Knowledge Discovery from Data* 18, 3 (Dec. 2023), 1–55. <https://doi.org/10.1145/3628601>
- [42] Mahmudur Rahman, Mansurul Alam Bhuiyan, and Mohammad Al Hasan. 2014. Graft: An Efficient Graphlet Counting Method for Large Graph Analysis. *IEEE Transactions on Knowledge and Data Engineering* 26, 10 (Oct. 2014), 2466–2478. <https://doi.org/10.1109/tkde.2013.2297929>
- [43] Matteo Riondato and Eli Upfal. 2018. ABRA: Approximating Betweenness Centrality in Static and Dynamic Graphs with Rademacher Averages. *ACM Transactions on Knowledge Discovery from Data* 12, 5 (July 2018), 1–38. <https://doi.org/10.1145/3208351>
- [44] Matteo Riondato and Fabio Vandin. 2018. MiSoSouP: Mining Interesting Subgroups with Sampling and Pseudodimension. In *Proceedings of the 24th ACM SIGKDD International Conference on Knowledge Discovery & Data Mining (KDD '18)*. ACM. <https://doi.org/10.1145/3219819.3219989>
- [45] Ryan Rossi and Nesreen Ahmed. 2015. The Network Data Repository with Interactive Graph Analytics and Visualization. *Proceedings of the AAAI Conference on Artificial Intelligence* 29, 1 (March 2015). <https://doi.org/10.1609/aaai.v29i1.9277>
- [46] Ryan A. Rossi, Nesreen K. Ahmed, Aldo Carranza, David Arbour, Anup Rao, Sungchul Kim, and Eunye Koh. 2019. Heterogeneous Network Motifs. (Jan. 2019). <https://doi.org/10.48550/ARXIV.1901.10026> arXiv:1901.10026 [cs.SI]
- [47] Ryan A. Rossi, Anup Rao, Tung Mai, and Nesreen K. Ahmed. 2020. Fast and Accurate Estimation of Typed Graphlets. In *Companion Proceedings of the Web Conference 2020*. ACM. <https://doi.org/10.1145/3366424.3382683>
- [48] Thomas Schank and Dorothea Wagner. 2005. Approximating Clustering Coefficient and Transitivity. *Journal of Graph Algorithms and Applications* 9, 2 (2005), 265–275. <https://doi.org/10.7155/jgaa.00108>
- [49] C. Seshadhri, Ali Pinar, and Tamara G. Kolda. 2014. Wedge sampling for computing clustering coefficients and triangle counts on large graphs. *Statistical Analysis and Data Mining: The ASA Data Science Journal* 7, 4 (may 2014), 294–307. <https://doi.org/10.1002/sam.11224>
- [50] Comandur Seshadhri and Srikanta Tirupura. 2019. Scalable Subgraph Counting: The Methods Behind The Madness. In *Companion Proceedings of The 2019 World Wide Web Conference (WWW '19)*. ACM, 1317–1318. <https://doi.org/10.1145/3308560.3320092>
- [51] Shai Shalev-Shwartz. 2014. *Understanding machine learning*. Cambridge University Press, Cambridge. Hier auch später erschienene, unveränderte Nachdrucke.
- [52] Shubhanshu Shekhar and Aaditya Ramdas. 2023. On the near-optimality of betting confidence sets for bounded means. <https://doi.org/10.48550/ARXIV.2310.01547>
- [53] Chuan Shi, Yitong Li, Jiawei Zhang, Yizhou Sun, and Philip S. Yu. 2017. A survey of heterogeneous information network analysis. *IEEE Transactions on Knowledge and Data Engineering* 29, 1 (Jan. 2017), 17–37. <https://doi.org/10.1109/tkde.2016.2598561>
- [54] Kijung Shin. 2017. WRS: Waiting Room Sampling for Accurate Triangle Counting in Real Graph Streams. In *2017 IEEE International Conference on Data Mining (ICDM)*. IEEE, 1087–1092. <https://doi.org/10.1109/icdm.2017.143>
- [55] Kijung Shin, Sejoon Oh, Jisu Kim, Bryan Hooi, and Christos Faloutsos. 2020. Fast, Accurate and Provable Triangle Counting in Fully Dynamic Graph Streams. *ACM Transactions on Knowledge Discovery from Data* 14, 2 (Feb. 2020), 1–39. <https://doi.org/10.1145/3375392>
- [56] Lorenzo De Stefani, Alessandro Epasto, Matteo Riondato, and Eli Upfal. 2017. TRIEST: Counting Local and Global Triangles in Fully Dynamic Streams with Fixed Memory Size. *ACM Transactions on Knowledge Discovery from Data* 11, 4 (June 2017), 1–50. <https://doi.org/10.1145/3059194>
- [57] Yizhou Sun and Jiawei Han. 2013. Mining heterogeneous information networks: a structural analysis approach. *ACM SIGKDD explorations newsletter* 14, 2 (2013), 20–28.
- [58] Charalampos E. Tsourakakis, U. Kang, Gary L. Miller, and Christos Faloutsos. 2009. DOULION. In *Proceedings of the 15th ACM SIGKDD international conference on Knowledge discovery and data mining*. ACM. <https://doi.org/10.1145/1557019.1557111>
- [59] Johan Ugander, Brian Karrer, Lars Backstrom, and Cameron Marlow. 2011. The Anatomy of the Facebook Social Graph. <https://doi.org/10.48550/ARXIV.1111.4503>
- [60] Pinghui Wang, Junzhou Zhao, Xiangliang Zhang, Zhenguo Li, Jiefeng Cheng, John C.S. Lui, Don Towsley, Jing Tao, and Xiaohong Guan. 2018. MOSS-5: A Fast Method of Approximating Counts of 5-Node Graphlets in Large Graphs. *IEEE Transactions on Knowledge and Data Engineering* 30, 1 (Jan. 2018), 73–86. <https://doi.org/10.1109/tkde.2017.2756836>
- [61] Duncan J. Watts and Steven H. Strogatz. 1998. Collective dynamics of 'small-world' networks. *Nature* 393, 6684 (jun 1998), 440–442. <https://doi.org/10.1038/30918>
- [62] Ian Waudby-Smith and Aaditya Ramdas. 2023. Estimating means of bounded random variables by betting. *Journal of the Royal Statistical Society Series B: Statistical Methodology* 86, 1 (Feb. 2023), 1–27. <https://doi.org/10.1093/jrssi/bqkad009>
- [63] Zhihao Wu, Youfang Lin, Jing Wang, and Steve Gregory. 2016. Link prediction with node clustering coefficient. *Physica A: Statistical Mechanics and its Applications* 452 (June 2016), 1–8. <https://doi.org/10.1016/j.physa.2016.01.038>
- [64] Junming Xu. 2001. *Topological Structure and Analysis of Interconnection Networks*. Springer US. <https://doi.org/10.1007/978-1-4757-3387-7>
- [65] Hao Yin, Austin R. Benson, and Jure Leskovec. 2018. Higher-order clustering in networks. *Physical Review E* 97, 5 (May 2018), 052306. <https://doi.org/10.1103/physreve.97.052306>
- [66] Hao Yin, Austin R. Benson, and Jure Leskovec. 2019. The Local Closure Coefficient: A New Perspective On Network Clustering. In *Proceedings of the Twelfth ACM International Conference on Web Search and Data Mining (WSDM '19)*. ACM. <https://doi.org/10.1145/3289600.3290991>
- [67] Hao Yin, Austin R. Benson, Jure Leskovec, and David F. Gleich. 2017. Local Higher-Order Graph Clustering. In *Proceedings of the 23rd ACM SIGKDD International Conference on Knowledge Discovery and Data Mining (KDD '17)*. ACM. <https://doi.org/10.1145/3097983.3098069>
- [68] M. Yuan. 2024. Central limit theorem for the average closure coefficient. *Acta Mathematica Hungarica* 172, 2 (March 2024), 543–569. <https://doi.org/10.1007/s10474-024-01416-z>
- [69] Chi Zhang, Wenkai Xiang, Xingzhi Guo, Baojian Zhou, and Deqing Yang. 2023. SubAnom: Efficient Subgraph Anomaly Detection Framework over Dynamic Graphs. In *2023 IEEE International Conference on Data Mining Workshops (ICDMW)*. IEEE, 1178–1185. <https://doi.org/10.1109/icdmw60847.2023.00154>
- [70] Hao Zhang, Yuanyuan Zhu, Lu Qin, Hong Cheng, and Jeffrey Xu Yu. 2017. *Efficient Local Clustering Coefficient Estimation in Massive Graphs*. Springer International Publishing, 371–386. [https://doi.org/10.1007/978-3-319-55699-4\\_23](https://doi.org/10.1007/978-3-319-55699-4_23)
- [71] Kangfei Zhao, Jeffrey Xu Yu, Hao Zhang, Qiyang Li, and Yu Rong. 2021. A Learned Sketch for Subgraph Counting. In *Proceedings of the 2021 International Conference on Management of Data (SIGMOD/PODS '21)*. ACM. <https://doi.org/10.1145/3448016.3457289>

## A MISSING PROOFS

PROOF OF LEMMA 3.2. First we let  $X_e$  be a Bernoulli random variable taking value 1 with probability  $p = 1/m$  and 0 otherwise for each edge  $e \in E$ . Then it follows that  $\mathbb{E}[X_e] = p$ , hence applying the linearity of expectation to Equation (1) we get

$$\begin{aligned}\mathbb{E}[X_q(v)] &= \mathbb{E}\left[\sum_{e \in E: v \in e} \frac{q|\Delta_e|X_e}{p} + (1-2q) \sum_{e \in E: v \in N_e} \frac{X_e}{p}\right] \\ &= \sum_{e \in E: v \in e} \frac{q|\Delta_e|\mathbb{E}[X_e]}{p} + (1-2q) \sum_{e \in E: v \in N_e} \frac{\mathbb{E}[X_e]}{p} \\ &= \sum_{e \in E: v \in e} q|\Delta_e| + (1-2q) \sum_{e \in E: v \in N_e} 1 \\ &= q\left(\sum_{e \in E: v \in e} |\Delta_e| - 2 \sum_{e=\{u,v\}: v \in N_u \cap N_v} 1\right) + \sum_{e \in E: v \in N_e} 1 \\ &= q(2|\Delta_v| - 2|\Delta_v|) + |\Delta_v| = |\Delta_v|.\end{aligned}$$

Where we used the fact that  $\sum_{e \in E: v \in e} |\Delta_e| = 2|\Delta_v|$  as each triangle  $\delta \in \Delta_v$  is counted twice and  $\sum_{e \in E: v \in N_e} 1 = |\Delta_v|$  as the number of triangles containing  $v \in V$  corresponds to the number of edges connecting two neighbors of  $v \in V$ .  $\square$

PROOF OF LEMMA 3.3. First observe that the function in Equation (2) is deterministic for any edge  $e \in E$ , i.e., the indicator functions are based on properties of the input graph  $G$ , and clearly  $G$  is fixed.

Taking the expectation of  $f_j(e)$  we have

$$\begin{aligned}\mathbb{E}[f_j(e)] &\stackrel{(A)}{=} \sum_{e \in E} \frac{\mathbb{E}[X_e]}{p} \frac{1}{|V_j|} \sum_{v \in V_j} \frac{a_q(v, e)}{|W_v^*|} \\ &\stackrel{(B)}{=} \frac{1}{|V_j|} \sum_{v \in V_j} \frac{1}{|W_v^*|} \sum_{e \in E} a_q(v, e) \\ &\stackrel{(C)}{=} \frac{1}{|V_j|} \sum_{v \in V_i} \psi_v = \frac{1}{|V_j|} \sum_{v \in V_j} \psi_v = \Psi_j.\end{aligned}$$

Where (A) comes from the linearity of expectation, (B) comes from  $\mathbb{E}[X_e] = p$ , by swapping the summations, and the fact that  $1/|W_v^*|$  does not depend on  $e \in E$  for any of nodes  $v \in V_i, i = 1, \dots, k$ , and (C) by noting that

$$\sum_{e \in E} a_q(v, e) = \sum_{e \in E: v \in e} q|\Delta_e| + (1-2q) \sum_{e \in E: v \in N_e} 1 = |\Delta_v|$$

from the proof of Lemma 3.2, concluding therefore the proof as  $|\Delta_v|/|W_v^*| = \psi_v$ .  $\square$

PROOF OF LEMMA 3.4. From Lemma 3.3 it holds that for each edge  $e \in E$  and each function  $f_j(e)$ , it is  $\mathbb{E}[f_j(e)] = \Psi_j$ , where  $\mathbb{E}[\cdot]$  is over a random edge  $e \in E$ . After noting that by definition  $f_j = \frac{1}{s} \sum_{e \in S} f_j(e)$ , the result follows by the linearity of expectation and  $|S| = s$ .  $\square$

PROOF OF LEMMA 3.5. First note that  $f_j$  in output to Algorithm 1 is the sample average over  $s$  i.i.d. random variables

$$f_j(e) = \sum_{e \in E} \frac{X_e}{p} \frac{1}{|V_i|} \sum_{v \in V_i} \frac{a_q(v, e)}{|W_v^*|}. \quad (4)$$

Therefore to bound the variance, note

$$\text{Var}\left[\frac{1}{s} \sum_{i=1}^s f_j(e)\right] = \frac{1}{s^2} \sum_i \text{Var}[f_j(e)] \leq \frac{\hat{\sigma}^2}{s}. \quad (5)$$

Where  $\hat{\sigma}^2$  is a bound on the variance on  $f_j(e)$ , we used the fact that the variables are i.i.d. and that  $\text{Var}[cX] = c^2 \text{Var}[X]$  for a random variable  $X$  and a constant  $c$ . We now bound the variance of  $f_j(e)$ . Recall that

$$\text{Var}[X] = \mathbb{E}[X^2] - (\mathbb{E}[X])^2, \quad (6)$$

hence,

$$\begin{aligned}\mathbb{E}[f_j(e)^2] &= \mathbb{E}\left[\sum_{e_1 \in E} \sum_{e_2 \in E} \frac{X_{e_1} X_{e_2}}{p^2} \frac{1}{|V_j|} \sum_{v_1 \in V_j} \frac{a_q(v_1, e_1)}{|W_{v_1}^*|} \frac{1}{|V_j|} \sum_{v_2 \in V_j} \frac{a_q(v_2, e_2)}{|W_{v_2}^*|}\right] \\ &\stackrel{(A)}{=} \sum_{e_1 \in E} \sum_{e_2 \in E} \frac{\mathbb{E}[X_{e_1} X_{e_2}]}{p^2} \frac{1}{|V_j|} \sum_{v_1 \in V_j} \frac{a_q(v_1, e_1)}{|W_{v_1}^*|} \frac{1}{|V_j|} \sum_{v_2 \in V_j} \frac{a_q(v_2, e_2)}{|W_{v_2}^*|} \\ &\stackrel{(B)}{\leq} \frac{1}{p} \frac{1}{|V_j|^2} \sum_{e_1 \in E} \sum_{v_1 \in V_j} \frac{a_q(v_1, e_1)}{|W_{v_1}^*|} \sum_{v_2 \in V_j} \sum_{e_2 \in E} \frac{a_q(v_2, e_2)}{|W_{v_2}^*|} \\ &\stackrel{(C)}{=} \frac{1}{p} \frac{1}{|V_j|^2} \sum_{e_1 \in E} \sum_{v_1 \in V_j} \frac{a_q(v_1, e_1)}{|W_{v_1}^*|} \sum_{v_2 \in V_j} \psi_{v_2} = \frac{1}{p} \left( \frac{1}{|V_j|} \sum_{v \in V_j} \psi_v \right)^2.\end{aligned}$$

Step (A) follows from the linearity of expectation, step (B) from the fact that  $\mathbb{E}[X_{e_1} X_{e_2}] \leq \mathbb{E}[X_{e_1}] = p$  noting that such random variables are 0-1 variables and for the events  $I \doteq "X_{e_1} = 1"$ , and  $I' \doteq "X_{e_2} = 1"$  it holds  $I \subseteq I'$ , and (C) follows from the same argument used in the proof of Lemma 3.3. The final claim follows by combining the above result with Equations (6) and (5), and the fact that  $f_j(e)$  is an unbiased estimator of the triadic measure over each partition  $j \in [k]$  (Lemma 3.3).  $\square$

PROOF OF THEOREM 3.8. We now show that  $\text{PD}(\mathcal{F}) = \text{VC}(\mathcal{H} \times [a, b], \mathcal{F}^+)$  is bounded by  $\lceil \log_2 \hat{\chi} \rceil + 1$ . Let  $\text{VC}(\mathcal{H} \times [a, b], \mathcal{F}^+) = \zeta$  be the size of the largest set of elements of the space  $\mathcal{H} \times [a, b]$  that can be shattered by the range-set  $\mathcal{F}^+$ , and let  $Q$  be the shattered set attaining such size, that is  $0 < |Q| = \zeta$ . Without loss of generality  $Q$  contains one element  $a = (e, x)$  for some  $e \in E$  and  $x > 0$  (note that  $x$  needs to be strictly greater than 0 otherwise the set  $Q$  cannot be shattered, see Lemma B.3), and furthermore note that there cannot be another element in  $Q$  of the form  $a = (e, y)$  for  $y \neq x$  (see Lemma B.2). There exist therefore  $2^{\zeta-1}$  distinct and non-empty subsets of  $Q$  containing the element  $a$  that we label as  $Q_1, \dots, Q_{2^{\zeta-1}}$ , since the set  $Q$  is shattered by  $\mathcal{F}^+$ . This implies therefore that there are  $R_1, \dots, R_{2^{\zeta-1}}$  ranges for some partitions  $V_j, j = 1, \dots, k$  for which it holds  $Q_i = Q \cap R_i$  with  $i = 1, \dots, 2^{\zeta-1}$ , by the definition of  $Q$ . Given an edge  $e$  from  $\mathcal{H} = E$ , an element of the form  $(e, x)$  can belong to at most  $\hat{\chi}$  distinct ranges, which is easy to see by the following argument: (1) for a function  $f_j(e)$  of a partition  $j = 1, \dots, k$  to be non-zero it should hold that there exists a node  $v \in V_j$  such that  $v \in \delta, \delta \in \Delta_e$  and (2) for an edge  $e = \{u, v\}$  it holds  $|\Delta_e| \leq \min\{d_u, d_v\}$  and further  $\Delta_e = \{\{u, v\} \cup \{w\} : (N_u \setminus \{v\}) \cap (N_v \setminus \{u\})\}$  implying that all the nodes forming a triangle with edge  $e = \{u, v\}$  should be in the neighborhood of the node with minimum degree among  $u$  and  $v$ . Therefore for a fixed edge



---

**Algorithm 2:** FindThreshold

---

**Input:**  $G = (V, E)$  with  $|V| = n$ .

**Output:** Value of the small-node degree threshold  $\beta$ .

```

1  $D = (0, \dots, 0) \in \mathbb{R}^{n-2}; \beta \leftarrow 2; T \leftarrow 0;$ 
2 for  $v \in V$  do  $D_{d_v} \leftarrow D_{d_v} + 1;$ 
3 while  $T < c|V|$  do
4    $T \leftarrow \beta^2 D_\beta;$ 
5    $\beta \leftarrow \beta + 1;$ 
6 return  $\beta - 1;$ 

```

---

$e = \{u, v\}$  at most  $\chi_z$  where  $z = \arg \min\{d_u, d_v\}$  distinct functions  $f_j(e)$  can have non-zero values. Hence the element  $a = (e, x) \in Q$  can be contained in at most  $\widehat{\chi}$  ranges, therefore

$$2^{\zeta-1} \leq \widehat{\chi} \implies \zeta \leq \lfloor \log_2 \widehat{\chi} \rfloor + 1.$$

□

**PROOF OF COROLLARY 3.10.** First we consider the case where  $q = 0$ . By a similar argument to the proof of Theorem 3.8 consider an element of the form  $e = (u, x)$  in the shattered set  $Q$  such that  $|Q| = \zeta$ , then the two nodes forming the edge  $e = \{u, v\}$  do not contribute to the functions  $f_j(e)$  for the partitions they belong to, that is  $2^{\zeta-1} \leq \widehat{\chi}'$ , taking the logarithm yields the claim. While for  $q = 1/2$  it can only be that at most two partitions (if  $k \geq 2$ ) have  $f_j(e) > 0$  and hence  $\widehat{\chi}' \leq 2$  implying that  $\zeta \leq 2$ . □

**PROOF OF COROLLARY 3.9.** Consider a star graph  $G = (V, E)$  over  $n$  nodes, then in such case  $\widehat{\chi} = 1$  as for each edge  $e = \{u, v\} \in E$  it holds that  $\min\{d_u, d_v\} = 1$ , hence by Proposition 3.8:  $\zeta \leq \lfloor \log_2 1 \rfloor + 1 = 1$ . □

**PROOF OF THEOREM 3.12.** To prove the claim we bound the probability of failure of TRIAD, that is let  $F$  be the event that TRIAD's guarantees do not hold. We now show  $\mathbb{P}[F] \leq \eta$ . Clearly if this is the case, then TRIAD succeeds with probability at least  $1 - \eta$ .

Let us define the following events:

- $F_1 = s \geq s_{\max}$  and there exists  $j \in [k]$  such that  $|f_j - \Psi_j| > \varepsilon_j$ ; and
- $F_2 = s < s_{\max}, \widehat{\varepsilon}_j \leq \varepsilon_j$ , for each  $j \in [k]$ , and there exists  $j \in [k]$  such that  $|f_j - \Psi_j| > \varepsilon_j$ .

These are the two conditions under which Algorithm 1 fails to report sufficiently accurate estimates, and under which its guarantees do not hold for the confidence intervals built around  $f_j$ , for  $j \in [k]$  as from the statement. By the combination of Theorem 3.8 and 3.6 then for TRIAD it holds that  $\mathbb{P}[F_1] \leq \eta/2$ , next consider  $\widehat{\varepsilon}_j$  to be computed through Theorem 3.11 at each iteration  $i$  using  $\eta' = \eta/2^{i+1}$  then by a union bound over the possible (infinite) iterations [10, 41] it holds that  $\mathbb{P}[F_2] \leq \eta/2$ . Hence, the failure probability of TRIAD  $\mathbb{P}[F_1 \cup F_2] \leq \mathbb{P}[F_1] + \mathbb{P}[F_2] \leq \eta/2 + \eta/2 \leq \eta$ , yielding the claim. □

**PROOF OF LEMMA 3.13.** Clearly  $\frac{1}{c-1} \sum_{e \in S} (f_j(e) - f_j)^2$  is an unbiased estimator of the variance of each function  $f_j$  for  $|S| = c$ , then notice that  $f_j = \frac{m}{c|V_j|} (\sum_e a_j(e) + q \sum_e b_j(e))$  and therefore

$$(f_j(e) - f_j)^2 = \frac{m^2}{|V_j|^2} [\hat{a}_j(e)^2 + q \hat{a}_j(e) \hat{b}_j(e) + q^2 \hat{b}_j(e)^2], \text{ hence}$$

$$\begin{aligned} \widehat{V}_q(f_j) &= \frac{m^2}{(c-1)|V_j|^2} \left( \sum_{e \in S} A_j + q B_j + C_j q^2 \right) \\ &= \frac{m^2}{(c-1)|V_j|^2} \left( \sum_{e \in S} \hat{a}_j(e)^2 + q \sum_{e \in S} \hat{a}_j(e) \hat{b}_j(e) + q^2 \sum_{e \in S} \hat{b}_j(e)^2 \right) \\ &= \frac{1}{(c-1)} \sum_{e \in S} (f_j(e) - f_j)^2 \end{aligned}$$

□

**PROOF OF LEMMA 3.14.** First note that  $\widehat{V}_q(f_j)$  is an unbiased estimate of  $\text{Var}[f_j]$ , additionally given that  $\widehat{V}_q(f_j)$  has bounded range, i.e., it is a finite sum over bounded terms. Hence, it exists a value  $B_q$  for each value of  $q$  such that  $\widehat{V}_q(f_j) \leq B_q$  therefore by Hoeffding's inequality (i.e., Theorem B.4) it holds  $\varepsilon' = B_q \sqrt{\frac{\log(2k/\eta')}{2|S|}}$ , for any bound on the error probability  $\eta'$ . □

**PROOF OF LEMMA 3.15.** Recall that for each partition  $j = 1, \dots, k$ , and each edge  $e \in E$  it holds that

$$f_j(e) = \frac{1}{p} \frac{1}{|V_i|} \sum_{v \in V_i} \frac{a_q(v, e)}{|W_v^*|}.$$

First notice that for a fixed edge  $e = \{u, v\} \in E$  the only nodes that can form a triangle with edge  $e \in E$  are those nodes such that  $w \in (\mathcal{N}_u \cap \mathcal{N}_v)$  for which it clearly holds that  $(\mathcal{N}_u \cap \mathcal{N}_v) \subseteq \mathcal{N}_z$  where  $z = \arg \min\{d_u, d_v\}$ , and further  $|\Delta_e| \leq d_z$ . Then recall that by definition  $a_q(v, e) = q|\Delta_e|1[v \in e] + (1 - 2q)1[v \in \mathcal{N}_e]$ , hence we have  $q|\Delta_e|1[w \in e] \leq qd_z$  for both the two nodes  $u, v \in e$  and

$$(1 - 2q)1[w \in \mathcal{N}_e] \leq (1 - 2q) \text{ for } w \in \mathcal{N}_z.$$

Therefore for each partition  $V_j$  we have that

$$f_j(e) \leq \frac{1}{p} \frac{1}{|V_i|} \left( \sum_{v \in V_i, v \in e} \frac{qd_z}{|W_v^*|} + \sum_{v \in V_i, v \in \mathcal{N}_z} \frac{(1 - 2q)}{|W_v^*|} \right).$$

which follows by the fact that  $f_j(e)$  is the sum of non-negative terms, clearly  $f_j(e) \leq \max_e \{f_j(e)\} = R_j$  as computed by the algorithm, the final result follows from the definition of  $p = 1/m$ . Finally the fact that  $\lfloor \log_2 \widehat{\chi} \rfloor + 1$  is an upper bound to the pseudo-dimension associated to the functions  $f_j$ , for  $j \in [k]$ , follows from Proposition 3.8 □

## B AUXILIARY THEORETICAL RESULTS

**LEMMA B.1 ([13]).** Given a graph  $G = (V, E)$  with  $n$  nodes and  $m$  edges, then

$$\sum_{\{u, v\} \in E} \min\{d_u, d_v\} \leq 2\xi m,$$

where  $\xi$  corresponds to the arboricity of the graph  $G$ , i.e., the minimum number of edge disjoint spanning-forests required in which  $G$  can be decomposed.

**LEMMA B.2 ([44]).** If  $B \subseteq \mathcal{H} \times [a, b]$  is shattered by  $\mathcal{F}^+$ , it may contain at most one element  $(e, x) \in \mathcal{H} \times [a, b]$  for each  $e \in \mathcal{H}$ .

**LEMMA B.3 ([44]).** If  $B \subseteq \mathcal{H} \times [a, b]$  is shattered by  $\mathcal{F}^+$ , it cannot contain any element of the form  $(e, a) \in \mathcal{H} \times [a, b]$  for any  $e \in \mathcal{H}$ .

---

**Algorithm 4: Fixq**

---

**Input:**  $G = (V, E), \mathcal{V}, |W_v^*|_{v \in V}, q$ , sample size  $c$ .  
**Output:** Terms  $A_j, B_j, C_j, j \in [k]$ .

```

1  $S \leftarrow \text{UniformSample}(E, c);$  //  $|S| = c$ 
2 for  $e \in S$  do
3    $a_j(e) \leftarrow \sum_{v \in V_j, v \in \mathcal{N}_e} 1/|W_v^*|;$ 
4    $b_j(e) \leftarrow \sum_{v \in V_j, v \in \mathcal{N}_e} |\Delta_e|/|W_v^*| + \sum_{v \in V_j, v \in \mathcal{N}_e} 1/|W_v^*|;$ 
5    $\bar{a} \leftarrow \bar{a} + a_j(e);$ 
6    $\bar{b} \leftarrow \bar{b} + b_j(e);$ 
7 for  $e \in S$  do
8    $\hat{a}_j(e) \leftarrow a_j(e) - \bar{a}/c;$ 
9    $\hat{b}_j(e) \leftarrow b_j(e) - \bar{b}/c;$ 
10 for  $j \leftarrow 1$  to  $k$  do
11    $A_j \leftarrow \sum_{e \in S} \hat{a}_j(e)^2;$ 
12    $B_j \leftarrow \sum_{e \in S} 2\hat{a}_j(e)\hat{b}_j(e);$ 
13    $C_j \leftarrow \sum_{e \in S} \hat{b}_j(e)^2;$ 
14 return  $A_j, B_j, C_j, j \in [k];$ 

```

---



---

**Algorithm 3: UpperBounds**

---

**Input:**  $G = (V, E), \mathcal{V}, |W_v^*|_{v \in V}, q$ .  
**Output:** Upper bounds:  $\zeta, R_1, \dots, R_k$ .

```

1  $\mathbf{r}_v \leftarrow (0, \dots, 0) \in \mathbb{R}^k; \chi_v \leftarrow 0$  for each  $v \in V$ ;
2 for  $v \in V$  do
3   foreach  $w \in \mathcal{N}_v$  do
4      $\mathbf{r}_v[j] \leftarrow \mathbf{r}_v[j] + \frac{(1-2q)}{|W_w^*|}$  such that  $w \in V_j$ ;
5    $\chi_v \leftarrow |\{j : w \in V_j \text{ and } w \in (\mathcal{N}_v \cup \{v\})\}|;$ 
6  $R_i \leftarrow 0$  for each  $i = 1, \dots, k; \hat{\chi} \leftarrow 0$ ;
7 foreach  $e = (u, v) \in E$  do
8    $z \leftarrow \arg \min\{d_u, d_v\};$ 
9   foreach  $r_j \in \mathbf{r}_z$  do
10     $\hat{R}_j \leftarrow r_j + q \frac{d_z}{|W_u^*|} \mathbf{1}[u \in V_j] + q \frac{d_z}{|W_v^*|} \mathbf{1}[v \in V_j];$ 
11     $R_j \leftarrow \max\{R_j, \hat{R}_j \frac{m}{|V_j|}\};$ 
12    $\hat{\chi} \leftarrow \max\{\hat{\chi}, \zeta_z\};$ 
13 return  $\lfloor \log_2 \hat{\chi} \rfloor + 1, R_1, \dots, R_k;$ 

```

---

**THEOREM B.4 (Hoeffding Bound [35]).** Let  $X_1, \dots, X_s$  be  $s$  independent random variables such that for all  $i = 1, \dots, s$ ,  $\mathbb{E}[X_i] = \mu$  and  $\mathbb{P}[X_i \in [a, b]] = 1$ . Then,

$$\mathbb{P}\left(\left|\frac{1}{s} \sum_{i=1}^s X_i - \mu\right| \geq \varepsilon\right) \leq 2 \exp(-2s\varepsilon^2/(b-a)^2).$$

## C MISSING SUBROUTINES

### C.1 Upper-bounds computation

Algorithm 3 details the procedure used to compute an upper bound to the range of functions  $f_j(e)$  for each of the possible sampled edges  $e \in E$  and partitions  $j \in [k]$ . The main idea is to first iterate through all the nodes maintaining a vector of size  $k$  (lines 1-4). Each entry in a vector is then used to compute an upper bound on the

range of  $f_j(e)$ , for  $j \in [k]$ , by iterating all edges  $e \in E$  (lines 6-11). For each edge  $e \in E$  we consider the vector corresponding to the node with minimum degree over  $e \in E$  to obtain the upper bounds  $R_j$ , for  $j \in [k]$  (line 8).

**Time complexity.** Next we analyze the time complexity of Algorithm 3, showing that in practice it is bounded by  $O(m)$ . First, computing the vectors  $\mathbf{r}_v$ , for  $v \in V$ , requires at most  $O(m)$  by the handshaking lemma. Next, the algorithm iterates the vectors  $\mathbf{r}_z, z \in V$  for all  $z$  corresponding to the minimum degree nodes over all edges  $e \in E$ . By storing only the non-zero entries over vectors  $\mathbf{r}_z, z \in V$ , the total non-zero entries are bounded by  $O(k)$  and by  $O(d_z)$ . Consider the bound  $O(k)$  then the time complexity of Algorithm 3 is bounded by  $O(km)$ , otherwise by Lemma B.1, the bound is  $O(\xi m)$ , where  $\xi$  is the arboricity of  $G$ . For practical values of  $k$ , i.e., when  $k$  is a large constant, the above bound is linear in  $m$ . Also note that if  $k \geq d_{\max}$  where  $d_{\max}$  is the maximum degree of a node in  $G$  then we can avoid iterating all entries in  $\mathbf{r}_z, z \in V$ , and use a tight deterministic upper bound on each  $f_j$  reducing the time complexity  $O(\xi m)$  to  $O(m)$ , yielding linear complexity again (see Section 3.3.1).

### C.2 Variance estimation

The procedure that we use to estimate the variance of the random variables  $f_j$  is detailed in Algorithm 4.

### C.3 Filtering small-degree nodes

In this section we briefly show that filtering small degree nodes, as described in Section 3.4.3, yields no estimation error for TRIAD.

**LEMMA C.1.** Let  $v \in V$  and  $|\Delta_v^L|$  be the counts returned for node  $v$  by Algorithm 5, and  $G'$  be the filtered graph of the input graph  $G$ . Then  $|\Delta_v| = |\Delta_v^L| + |\Delta_v'|$ , where  $\Delta_v'$  (resp.  $\Delta_v$ ) is the set of triangles containing node  $v \in V'$  in  $G'$  (resp.  $G$ ).

**PROOF.** Pick an arbitrary node  $v \in V'$  and let  $\Delta_v$  be the set of triangles containing node  $v \in V'$  in  $G = (V, E)$ . Then the set  $\Delta_v = \{\delta_1, \dots, \delta_{|\Delta_v|}\}$  can be partitioned as follows, let  $\Delta_v^L = \{\delta \in \Delta_v : \text{it exists } w \in (V \setminus V') \text{ and } w \in \delta\}$  corresponding to the set of triangles containing at least one node removed from  $G$  by Algorithm 5 as from the statement, and  $\Delta_v' = \Delta_v \setminus \Delta_v^L$ . Therefore it follows that  $\Delta_v = \Delta_v^L \cup \Delta_v'$ , yielding the claim, as  $\Delta_v^L \cap \Delta_v' = \emptyset$ .  $\square$

Lemma C.1 allows us to safely remove small degree nodes while focusing on estimating the number of remaining coefficients  $\Psi_j$  in the filtered graph  $G'$ . The next lemma shows that if we obtain function  $f_j$  with respect to some slightly modified scores  $\Psi_j'$  we can recover  $|f_j - \Psi_j| \leq \varepsilon_j$ , for  $j \in [k]$  on the original graph  $G$ , i.e., the desired output.

**COROLLARY C.2.** Let  $\psi_v' = \frac{|\Delta_v'|}{|W_v^*|}$  where  $W_v^*$  refers to the graph  $G$  (i.e., not preprocessed) and  $\Psi_j' = 1/|V_j| \sum_{v \in V_j} \psi_v'$  then if  $f_j'$  is an estimate such that  $|f_j' - \Psi_j'| \leq \varepsilon_j$ , for  $j \in [k]$  in  $G'$  then  $f_j = f_j' + \frac{1}{|V_j|} \sum_{v \in V_j} \frac{|\Delta_v^L|}{|W_v^*|}$  is such that  $|f_j - \Psi_j| \leq \varepsilon_j$ , for  $j \in [k]$  in  $G$ .

**PROOF.** The proof directly follows from the definition of  $\psi_v$  which by Lemma C.1 can be written as  $\psi_v = \frac{|\Delta_v^L| + |\Delta_v'|}{|W_v^*|}$ . Hence,

---

**Algorithm 7:** SampleWedge [25, 49]

---

**Input:**  $G = (V, E), v \in V$ .**Output:** A wedge sampled uniformly at random from  $W_v^c$ .

```

1  $u_1 \leftarrow \text{Uniform}(\mathcal{N}_v)$ ;
2  $u_2 \leftarrow \text{Uniform}(\mathcal{N}_v \setminus \{u_1\})$ ;
3  $w \leftarrow \langle u_1, u_2 \rangle$ ;
4 return  $w$ ;
```

---



---

**Algorithm 8:** Sample2Path

---

**Input:**  $G = (V, E), v \in V$ .**Output:** A 2-path sampled uniformly at random from  $W_v^h$ .

```

1  $p_{u_1}, \dots, p_{u_{|d_v|}} \leftarrow \frac{d_{u_1}-1}{\sum_{u \in \mathcal{N}_v} (d_u-1)}, \dots, \frac{d_{u_{|d_v|}}-1}{\sum_{u \in \mathcal{N}_v} (d_u-1)}, u_i \in \mathcal{N}_v$ ;
2  $u_1 \leftarrow \text{Sample}(\mathcal{N}_v, p_i)$ ;
3  $u_2 \leftarrow \text{Uniform}(\mathcal{N}_{u_1} \setminus \{v\})$ ;
4  $w \leftarrow \langle u_1, u_2 \rangle$ ;
5 return  $w$ ;
```

---



---

**Algorithm 5:** Filter small-degree nodes

---

**Input:**  $G = (V, E)$ .**Output:** Filtered graph  $G' = (V', E')$ , counts  $|\Delta_v^L|$  for  $v \in V$ .

```

1  $V' \leftarrow V$ ;
2 foreach  $v \in V' : d_v = 1$  do
3    $V' \leftarrow V' \setminus \{v\}$ ;
4  $E' \leftarrow \text{Update}(E, V')$ ;
5  $\beta \leftarrow \text{FindThreshold}(G)$ ; //  $\Theta(n)$ 
6 foreach  $v \in V' : 2 \leq d(v) \leq \beta$  do
7   foreach  $\delta \in \Delta_v$  do
8     foreach  $w \in \delta$  do  $|\Delta_w^L| \leftarrow |\Delta_w^L| + 1$ ;
9    $V' \leftarrow V' \setminus v$ ;
10   $E' \leftarrow \text{Update}(E, V')$ ;
11 return  $G' = (V', E')$ ,  $|\Delta_v^L|$  for  $v \in V$ ;
```

---



---

**Algorithm 6:** WedgeSampler

---

**Input:**  $G = (V, E)$ , partitions  $V_i, \varepsilon_i, i = 1, \dots, k, \eta, \psi$ .**Output:**  $f(V_i) \in \Psi(V_i) \pm \varepsilon_i$  w.p.  $\geq 1 - \eta$ .

```

1  $\hat{\psi}_v \leftarrow 0, v \in V; s \leftarrow \lceil \frac{1}{2\varepsilon_i^2} \log(2k/\eta) \rceil$ ;
2 foreach  $i \leftarrow 1$  to  $k$  do
3    $S \leftarrow \emptyset$ ;
4   for  $j \leftarrow 1$  to  $s$  do
5      $v \leftarrow \text{Uniform}(V_i)$ ;
6     if  $\psi = \alpha$  then
7        $S \leftarrow S \cup \text{SampleWedge}(v)$ ;
8     else if  $\psi = \phi$  then
9        $S \leftarrow S \cup \text{Sample2Path}(v)$ ;
10  foreach  $w \in S : \text{"w = closed"}$  do
11     $f_i \leftarrow f_i + \frac{1}{s}$ ;
12 return  $f_i, i = 1, \dots, k$ ;
```

---

$f_j = \frac{1}{|V_j|} \sum_{v \in V_j} \psi_v = \frac{1}{|V_j|} \sum_{v \in V_j} \frac{|\Delta_v^L|}{|W_v^h|} + \frac{1}{|V_j|} \sum_{v \in V_j} \frac{|\Delta_v^L|}{|W_v^c|}$  hence by the definition of  $f_j'$ , and the fact that there is no error over the second term, the claim follows.  $\square$

The above result captures the fact that we can execute TRIAD on the processed graph  $G'$ , by only adopting  $W_v^*$ , for  $v \in V$ , from the original graph  $G$  without any loss on the guarantees over  $G$ , with negligible overhead (i.e., only  $O(n)$  total additional work).

The exact procedure for filtering small degree nodes is detailed in Algorithm 5.

## D BASELINES

The baseline considered is based on the state-of-the-art approach devised for estimating local clustering coefficients by sampling [49]. We denoted such algorithm by WedgeSampler. We present such baseline in Algorithm 6. Note that the WedgeSampler exactly coincides with the approach of Seshadhri et al. [49] when the considered metric is the clustering coefficient, in particular, such algorithm proceeds as follows: consider each partition independently  $V_i, i = 1, \dots, k$ : (i) uniformly sample a random node  $v$  from each partition  $V_i, i = 1, \dots, k$ ; (ii) for the sampled node, uniformly sample a wedge centered at the node and update an estimate if the wedge is closed, i.e., it forms a triangle; (iii) repeat such steps until concentration (i.e., for  $O(\varepsilon_i^{-2} \log(k/\eta))$ ). Such approach is based on the fact that a random sampled wedge from a node  $v \in V_i$  provides an unbiased estimate of  $\alpha_v$ . Inspired by such approach we designed a non trivial baseline for estimating the closure coefficient  $\phi_v$  for a node  $v \in V$ , which is based on uniformly sampling a wedge *headed* at  $v \in V$ , that is we uniformly sample  $w$  from  $W_v^h$ , which requires particular attention to avoid bias in the final sampling procedure, in particular we have the following.

**LEMMA D.1.** *Each wedge  $w \in W_v^h$  in output to Algorithm 8 is sampled uniformly at random from  $W_v^h$  for  $v \in V$ , and the probability that a sampled path is closed, i.e., forms a triangle with  $v \in V$  corresponds to  $\phi_v$ .*

**PROOF.** Let us compute the probability to sample a path  $w = \langle u_1, u_2 \rangle \in W_v^h$  of length-2 starting from a node  $v \in V$ ,

$\mathbb{P}[w = \langle u_1, u_2 \rangle \text{ is sampled}] = \mathbb{P}[u_1 \text{ is 1-st node}] \mathbb{P}[u_2 \text{ is 2-nd node}]$

$$= p_{u_1} \cdot p_{u_2} = \frac{d_{u_1}-1}{\sum_{u \in \mathcal{N}_v} (d_u-1)} \cdot \frac{1}{d_{u_1}-1} = \frac{1}{\sum_{u \in \mathcal{N}_v} (d_u-1)}$$

Therefore the 2-path  $w = \langle u_1, u_2 \rangle$  is sampled uniformly among all the  $\sum_{u \in \mathcal{N}_v} (d_u - 1)$  paths of length 2 headed at  $v \in V$ . To compute the probability that such path is closed, notice that a path can be closed only if  $\{u_1, u_2, v\} \in \Delta$ , that is if the three nodes form a triangle, hence

$$\mathbb{P}[w = \langle u_1, u_2 \rangle \text{ is closed}] = \frac{2|\Delta_v|}{\sum_{u \in \mathcal{N}_v} (d_u-1)} = \phi_v.$$

where we used the fact that each triangle contributes to two distinct wedges that can be sampled by Algorithm 8.  $\square$

**COROLLARY D.2.** *The output  $f_i$  of Algorithm 6 is unbiased and it holds that  $\mathbb{P}[|f_i - \Psi_i| \geq \varepsilon_i] \leq \eta$  simultaneously for all  $i = 1, \dots, k$ .*

PROOF. When Algorithm 7 is executed for the clustering coefficient  $\alpha$ , this immediately follows from the results of Seshadhri et al. [49]. While when Algorithm 7 is executed for the closure coefficient  $\phi$  we can write  $f_i$  as,

$$f_i = \frac{1}{s} \sum_{t=1}^s \sum_{v \in V} X_w^v$$

where  $X_w^v$  is an indicator random variable if the wedge  $w$  headed at  $v \in V$  sampled by the algorithm is closed, clearly  $\mathbb{P}[X_w^v = 1] = \frac{\phi_v}{|V_i|}$  as it is the results of the event that node  $v \in V_i$  is sampled (which occurs with probability  $1/|V_i|$ ) and that a closed wedge headed at  $v \in V_i$  is sampled that occurs with probability  $\phi_v$  by Corollary D.1, hence  $\mathbb{E}[f_i] = \Psi_i$ . The concentration of  $f_i$  follows by Hoeffding's bound (Theorem B.4) and the application of the union bound over the  $k$  partitions.  $\square$

## E PARAMETER SETTING

Following the discussion in Section 3.6, since TRIAD adapts both the parameter  $q$  and the bounds  $\hat{\epsilon}_j$  we found that best parameter setting is as follows:

- Setting the parameter  $C$  (the threshold defining the filtering of small-degree nodes) according to the degree distribution of the graph. That is, such that the minimum-degree of the nodes  $v \in V'$  in the remaining graph  $G'$  have degree  $\geq 10$  in the original graph  $G$  (note that they may have smaller degree in  $G'$ ). This helps to obtain a better bound for the values  $R_j$ , for  $j \in [k]$ .
- Setting the parameter  $\eta = 0.01$ , as it gives high probabilistic guarantees of success and it has little impact on the final sample size.
- Setting  $c$ , i.e., the sample size used to estimate the variance of the functions  $f_j$ , for  $j \in [k]$  and optimize the parameter  $q$  to a small constant, (we use  $c = 500$ ), therefore fixing the value of  $q$  becomes extremely efficient.
- Setting the parameter  $\theta$  controlling the geometric sample schedule  $s_i = \theta s_{i-1}$  to  $\theta = 1.4$ , in accordance with previous work [41, 43]. Often yielding good results in practice as shown in Section 4.
- Setting the parameters  $\epsilon_j = \epsilon \in (0.15, 0.05)$ , this is given by the fact that TRIAD's guarantees are adaptive. Hence, as from Section 4.3 it is often the case that TRIAD returns bounds  $\hat{\epsilon}_j$  much smaller than  $\epsilon_j$  (up to the order of  $10^{-4}$ ). This is clearly, another advantage of our algorithm  $\epsilon$ .

Concerning TRIAD-F we observe that it is often sufficient to set the sample size  $s = m/500$  where  $m$  is the number of edges in the graph  $G$ , to obtain empirical errors  $|f_j - \Psi_j|$  that are negligible, yielding also remarkably accurate relative approximations.

## F ADDITIONAL RESULTS

### F.1 Reproducibility

The code used for our experiments is available online (<https://github.com/iliesarpe/Triad>). Below we provide additional details on the setup of the experiments.

*F.1.1 Datasets.* All the datasets that we considered are available online, in particular we downloaded some of the largest graphs

from SNAP [30], and the network repository [45]. More in more detail,

- fb-CMU (<https://networkrepository.com/fb-CMU-Carnegie49.php>)
- SP (<https://snap.stanford.edu/data/soc-Pokec.html>)
- FR (<https://snap.stanford.edu/data/com-Friendster.html>)
- OR (<https://snap.stanford.edu/data/com-Orkut.html>)
- LJ (<https://snap.stanford.edu/data/soc-LiveJournal1.html>)
- BM (<https://networkrepository.com/bio-mouse-gene.php>)
- G500 (<https://networkrepository.com/graph500-scale23-ef16-adj.php>)
- GP ([https://snap.stanford.edu/data/gplus\\_combined.txt.gz](https://snap.stanford.edu/data/gplus_combined.txt.gz))
- PT (<https://networkrepository.com/proteins-all.php>)
- HW (<https://networkrepository.com/ca-hollywood-2009.php>)
- HG (<https://snap.stanford.edu/data/higgs-twitter.html>)
- BNH (<https://networkrepository.com/bn-human-BNU-1-0025919-session-1.php>)
- TW ([https://snap.stanford.edu/data/twitch\\_gamers.html](https://snap.stanford.edu/data/twitch_gamers.html))

Since we deal with simple and undirected graphs, we only performed standard pre-processing, i.e., removing self loops and parallel edges, and remapping nodes from  $1, \dots, n$ .

*F.1.2 Parameter and settings.* We further clarify all the parameter settings used in the various experiments. Note that all the scripts for reproducing the results are provided with the source code (i.e., containing also the parameters described hereby). This section is in addition to that.

- For the setting of Section 4.2: we do not set the values of the parameters  $\epsilon, \delta$ , as we used TRIAD-F. The value of  $C$  used for the optimization in Section 3.4 is fixed to 30 for all datasets but G500, BNH, BM where  $C = 100$ . As discussed in Section 4.2, we tested different values of  $s$  according to the size of the graph considered setting  $s=1\%$ ,  $s=2\%$ ,  $s=5\%$ . The value of the parameter  $q$  is optimized according to Section 3.3.3 and a total samples of 10% of  $s$ .
- For the setting in Section 4.3: we run all datasets with  $\epsilon = 0.075$  and  $\delta = 0.01$ . For each partition we obtain  $\hat{\epsilon}$  from TRIAD and we use it as input for the baselines. The value of  $C$  used for the optimization in Section 3.4 is fixed to 150 for all datasets but G500, GSH, BNH, BM where  $C = 500$ . The value of the parameter  $q$  is optimized according to Section 3.3.3 over a total of 500 sampled edges. The time limit was set to 10 minutes for all datasets but the largest/densest ones (i.e., G500, BNH, BM) where the time limit was set to 1 hour.
- For the setting of Section 4.5: we set  $\epsilon_j = \epsilon = 0.05$  for each  $j$  corresponding to a different community, and  $\eta = 0.01$ . The results shown, are over a single run.

*F.1.3 DBLP dataset.* Here we provide additional information on how we build the DBLP dataset. We used the DBLP dump referring to August 2024 (<https://dblp.org/xml/release/dblp-2024-08-01.xml.gz>), all the code to generate such data is reported in our repository. To classify the authors on each snapshot from Section 4.5, considering the following classification rule,

- We first consider the following fields represented by a set of conferences:

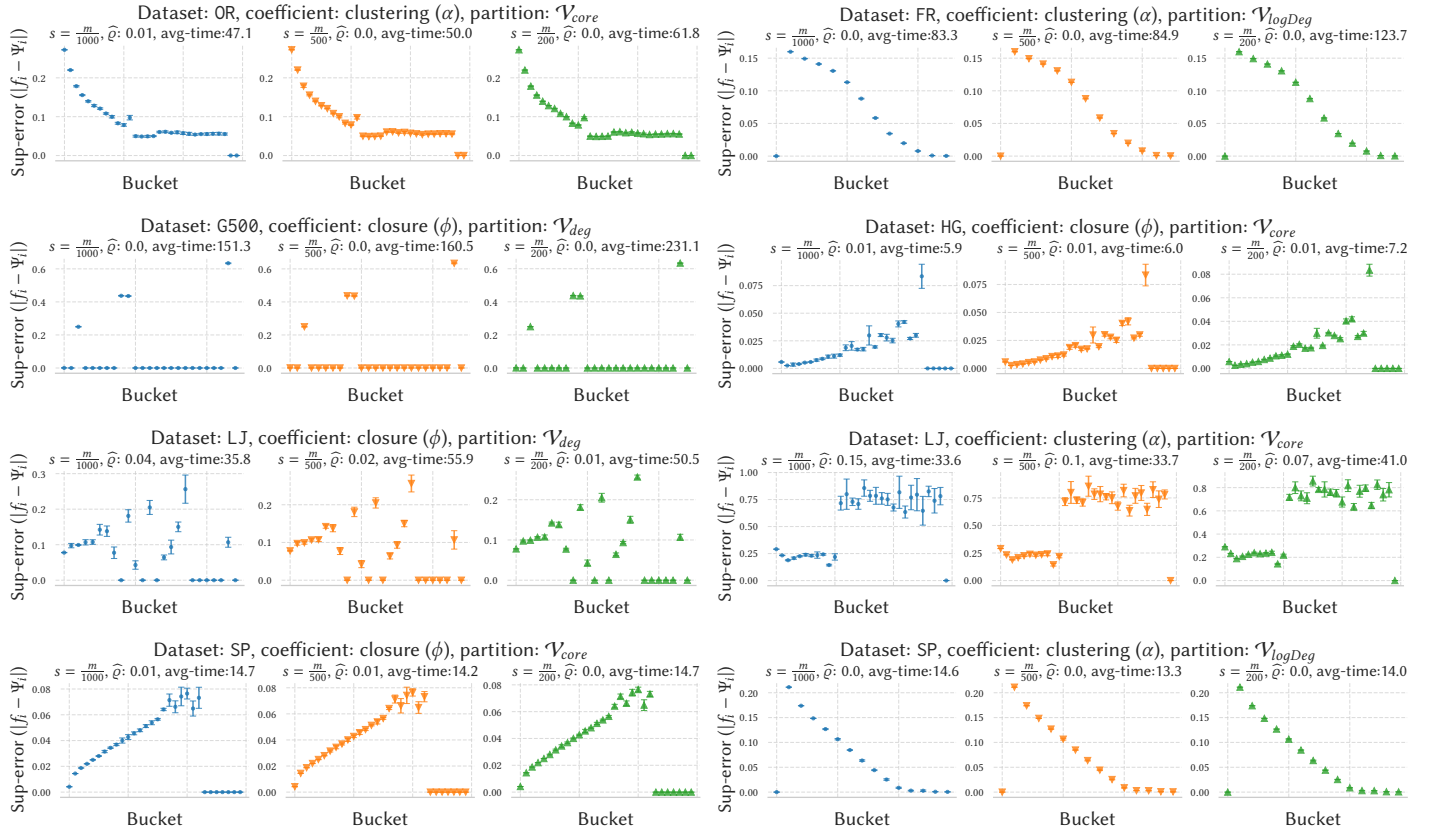


**Figure 9: Value  $\Psi_i$  and its maximum error ( $|f_i - \Psi_i|$ ) over five runs. We also report, the supremum error  $\hat{q} = \sup_{i \in [k]} |f_i - \Psi_i|$  and the average runtime over five independent runs across all buckets, for varying sample size ( $s \in \{1, 2, 5\}\%$  of the total edges  $m$ ).**

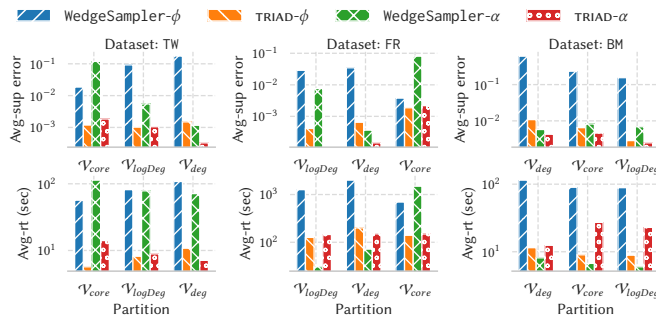


**Figure 10: Comparison of TRIAD and the base-lines WedgeSampler. For each dataset we show, (top plot): the average supremum error over all buckets over the various runs. (bottom): average runtime to perform an execution.**

- Data management: VLDB, PVLDB, SIGMOD, PODS, ICDE, PODC, SIGIR;
- Data mining: KDD, WWW, CIKM, SDM, DAMI, TKDD, TKDE, WSDM, SIGKDD;

- Machine learning: NIPS, ICML, ICLR, AAAI, IJCAI, AA-MAS;
- Theoretical computer science (TCS): STOC, FOCS, SODA, ITCS, ICALP, ISAAC, ESA, FOSSACS, STACS, COLT, MFCS, STACS;
- Computational biology: RECOMB, CIBB, ISMB, WABI, PSB;
- Software engineering: ASE, DEBS, ESEC, FSE, ESEM, ICPE, ICSE, ISSTA, MOBILESoft, MoDELS, CBSE, PASTE, SIG-SOFT;

- For each author we count the number of publication in the above fields, and assign the label according to field in which the author published most. If the author did not publish in any of the fields, we assign it to the “other” category.

We note that for some of the graphs that refer to years from 1970 to 1995, for some communities we have no information, i.e., the number of authors in such communities is 0. This is likely due to the classification above, and the set of conferences that we used to classify the authors, which started after the considered years. To obtain the score in Figure 7 we use TRIAD with  $\varepsilon = 0.05$  and  $\eta = 0.01$  on each dataset over a single run.

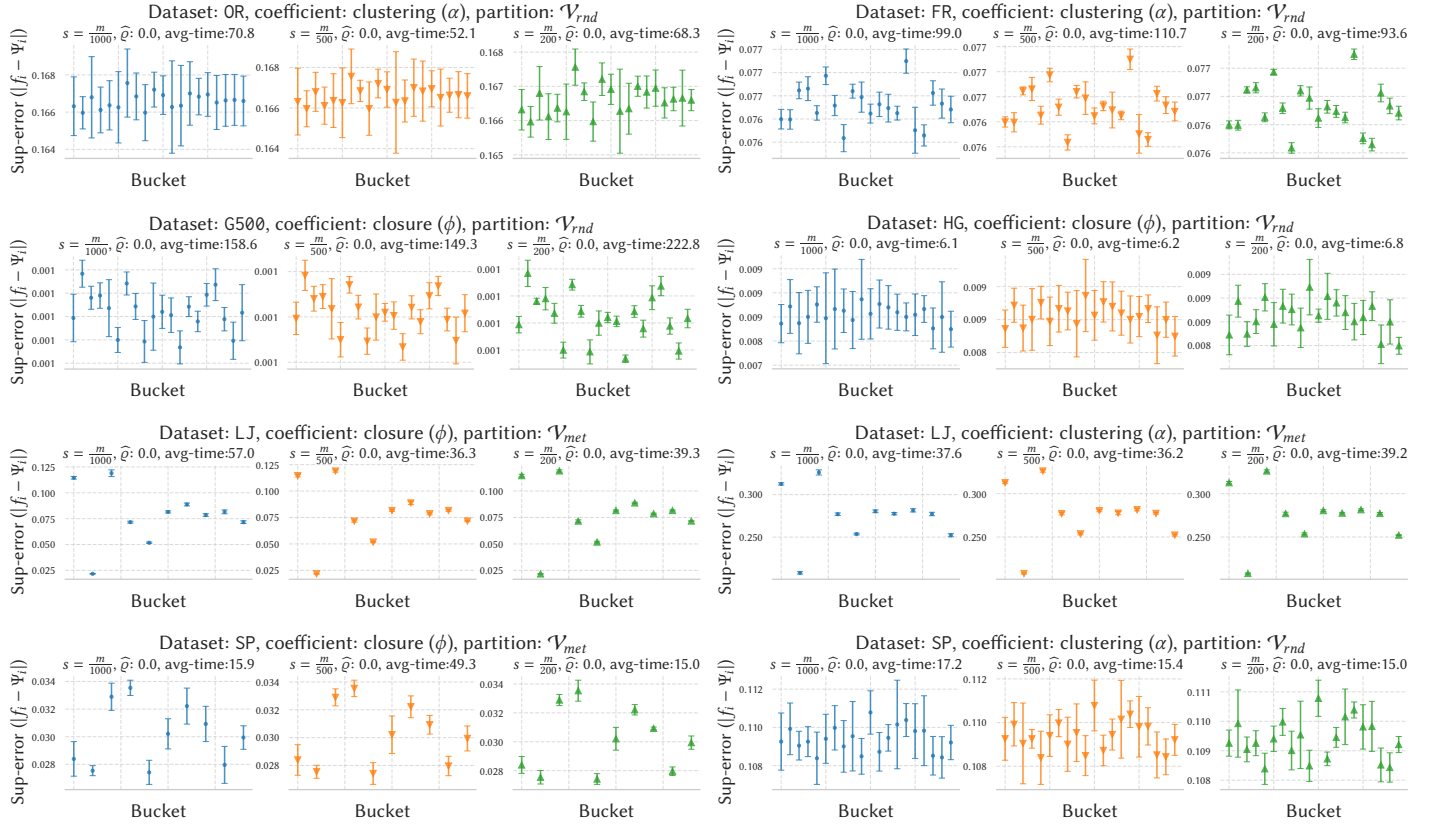


**Figure 11: Value  $\Psi_i$  and its maximum error ( $|f_i - \Psi_i|$ ) over five runs. We also report, the supremum error  $\hat{\varrho} = \sup_{i \in [k]} |f_i - \Psi_i|$  and the average runtime over five independent runs across all buckets, for varying sample size ( $s \in \{1, 2, 5\}\%$  of the total edges  $m$ ).**

## F.2 Extending the results of Section 4.2

Figure 9 reports additional configurations for the setting of the experiments in Section 4.2. Results follow similar trends to the ones already discussed.

Further, we also considered two additional partitions,  $\mathcal{V}_{rnd}$  and  $\mathcal{V}_{met}$ .  $\mathcal{V}_{rnd}$  is obtained by randomly assigning the nodes over  $k = 30$  random buckets and  $\mathcal{V}_{met}$  is obtained by using the METIS algorithm [24] with  $k = 10$  clusters, (we use PyMetis: <https://github.com/inducer/pymetis/tree/main>) First note that clearly under  $\mathcal{V}_{rnd}$  each value  $\Psi_i$  corresponds to an unbiased estimate of the value  $\Psi$  computed on the node-set  $V$ , i.e., the global average clustering or closure coefficient. Hence all such values are expected to be close. Results are reported in Figure 11, which confirm our observation, i.e., when considering  $\mathcal{V}_{rnd}$  all the values  $\Psi_i$  are close, and are also close to  $\bar{\alpha}$  or  $\bar{\phi}$  from Table 1. Overall the results support what we observed in Section 4.2 where a sample size of  $2\%$  is often sufficient to achieve a supremum error of the order of  $10^{-3}$ , yielding highly accurate estimates for all buckets.

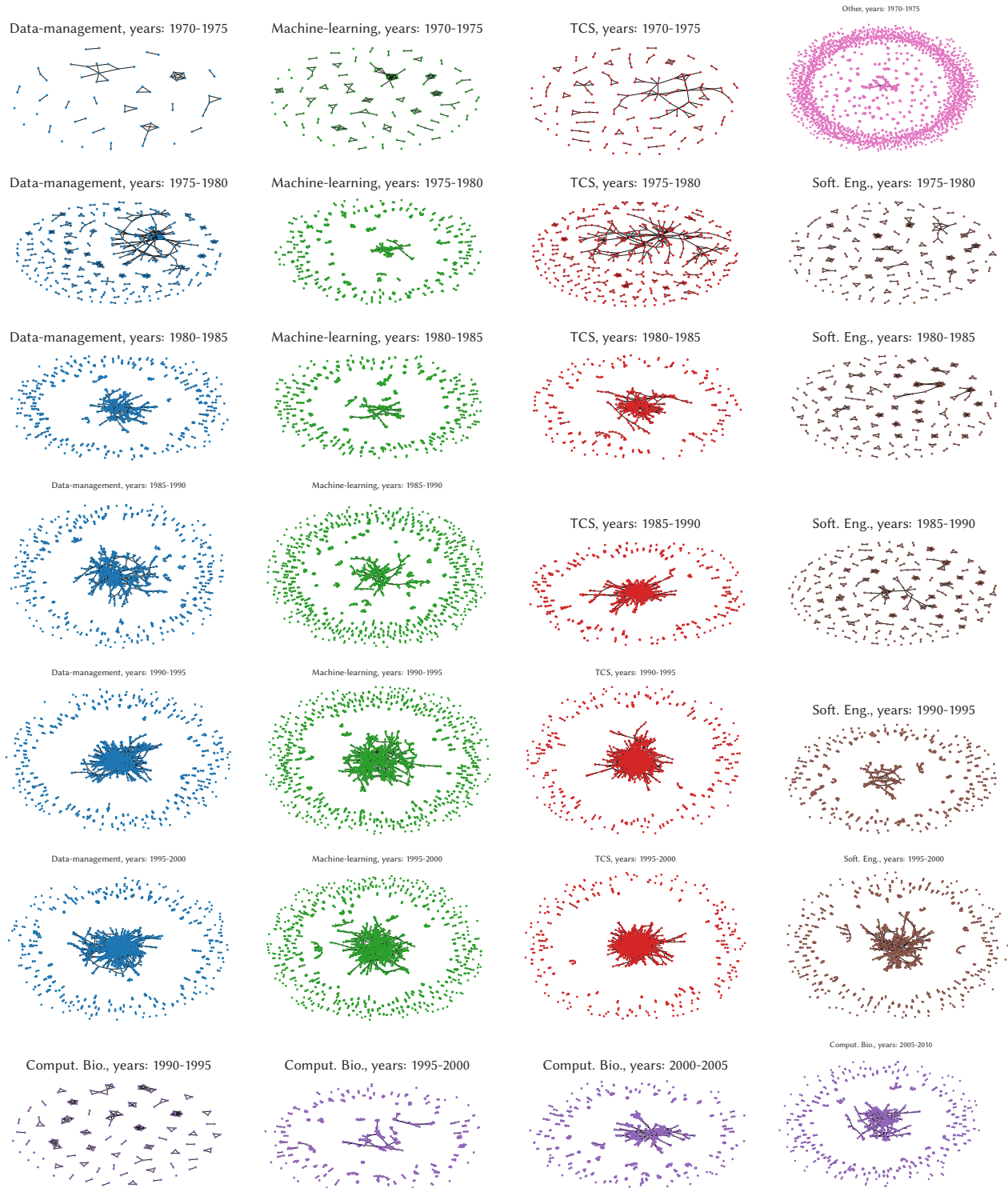
## F.3 Extending the results of Section 4.3

Figure 10 reports additional configurations for the setting of the experiments in Section 4.3. Also in this case, results follow similar trends to the ones already discussed.

## F.4 Extending the results of Section 4.5

Figure 12 reports additional visualization of the structure of the induced subgraphs considered in Section 4.5 and for which some representative examples were shown in Figure 8.

Figure 13 reports the degree distribution of the various authors in each category, to account for the relative of each category we report, for each bin  $[x_1, x_2]$  representing a range for the degrees of the various nodes the *fraction* of nodes attaining a value of their degree in the range  $[x_1, x_2]$ . We can observe that the data-mining category and the computational biology community both have similar degree distributions (e.g., years 1990-1995 or 2000-2005). Hence their very different values of the triadic coefficients, which can be seen in Figure 7 cannot be uniquely explained by the degree distribution. In fact, we believe such values to be related to the different high-order collaboration patterns, as captured by the community structures in Figure 12.



**Figure 12: Induced subgraphs by the various research communities over time. We select sufficiently small-sized subgraphs for ease of visualization.**





**Figure 13: Binned degree distribution of the various research categories over the DBLP graph. Y-axis is in log-scale for ease of visualization.**